Master Thesis of the University of Ulsan

The effect of stacking sequence and fabrication on mode I, mode II fracture toughness of glass fiber reinforced unsaturated polyester resin composites

The Graduate School

of the University of Ulsan

Department of Mechanical Engineering

Tian Gou

The effect of stacking sequence and fabrication on mode I, mode II fracture toughness of glass fiber reinforced unsaturated polyester resin composites

Supervisor: Professor Young-Jin Yum

A Dissertation

Submitted to

The Graduate School of the University of Ulsan

In partial Fulfillment of the Requirements

for the Degree of

Master of Engineering

By

Tian Gou

Department of Mechanical Engineering

Ulsan, Korea

May, 2019

GOU TIAN 의 공학박사학위 논문을 인준함

심사위원장 주석재 (인)

심사위원 천두만 (인)

심사위원 염영진 (인)

울산대학교 대학원

2019 년 5 월

The effect of stacking sequence and fabrication on mode I, mode II fracture toughness of glass fiber reinforced unsaturated polyester resin composites

This certifies that the master's thesis
of Tian Gou is approved by

_____
Committee Chair Prof. Chu Seok Jae

_____
Committee Member Prof. Chun Doo Man

_____
Committee Member Prof. Young Jin Yum

Department of Mechanical Engineering
Ulsan, Korea
May, 2019

ACKNOWLEDGEMENTS

First and foremost, I want to express my heartfelt gratitude to my advisor Professor Young-Jin Yum, whose patient guidance, valuable suggestions and constant encouragement in the academic studies. Without his invaluable help and generous encouragement, the present thesis would not have been accomplished.

Besides, I would like to thank to all the Professors in the school of Mechanical Engineering at University of Ulsan, thanks for their great knowledge that I have learned. I would also express my gratitude to the master committee members: Prof. Chu and Prof. Chun for their inspiring advice and helpful feedback to evaluate my work.

Last but not least, I would like to express my special thanks to my parents who have always been helping me out of difficulties and supporting without a word of complaint. I would also like to thank my girlfriend Xiaoxiao Song, for love and spiritual encouragement during these two years. I will do my best to let us have a better life.

University of Ulsan, Republic of Korea

May, 2019

Tian Gou

ABSTRACT

Glass fiber reinforced composites have been widely used as alternative materials for decades because of their better mechanical properties. Two types of glass fiber, chopped strand mat (M) and woven (W), were combined together by using unsaturated polyester resin (UPR) and different stacking sequence. Totally 6 stacking sequences were designed to investigate the effect of stacking sequence based on the tensile properties and fracture toughness as follows: $[M_4/M_4]$, $[W_4/W_4]$, $[M_4/W_4]$, $[M/W]_4$, $[M/W/M/W]_S$, $[W/M/W/M]_S$, and a Teflon film was inserted to the center layer as an initial crack during fracture test. The same stacking sequences were used to verify the optimum fabrication conditions such as vacuum, mixing with multi-walled carbon nanotubes (MWCNTs) into UPR. Several factors such as density, Young's modulus, Poisson's ratio and interlaminar fracture toughness of composites were calculated from the experiment data. From the result, the $[W/M/W/M]_S$ combination was founded to be the best stacking sequence based on these factors. Besides, the vacuum assistant and MWCNTs had a positive effect on fracture toughness in mode I and mode II tests. Consequently, the properly designed structure is recommended under different fabrication conditions.

CONTENTS

LIST OF FIGURES

LIST OF TABLES

ABBREVIATIONS

FRP: Fiber reinforced polymers

UPR: Unsaturated polyester resin

CSM: Chopped strand mat

W: Woven (roving)

MWCNTs: Multi-walled carbon nanotubes

MEKP: Methyl ethyl ketone peroxide

DCB: Double cantilever beam

ENF: End-notched flexural

ASTM: American Society for Testing and Materials

NPC: Non-Precracked

CC: Compliance calibration

CHAPTER 1:

Introduction

A composite material (also called a composition material or shortened to composite) is a material made from two or more constituent materials with significantly different physical or chemical properties, when combined, produce a material with characteristics different from the individual components. The individual components remain separate and distinct within the finished structure, differentiating composites from mixtures and solid solutions [1,2]. The straw and mud combined to form bricks were the earliest man-made composite materials used for building construction at around the 1,500 B.C.

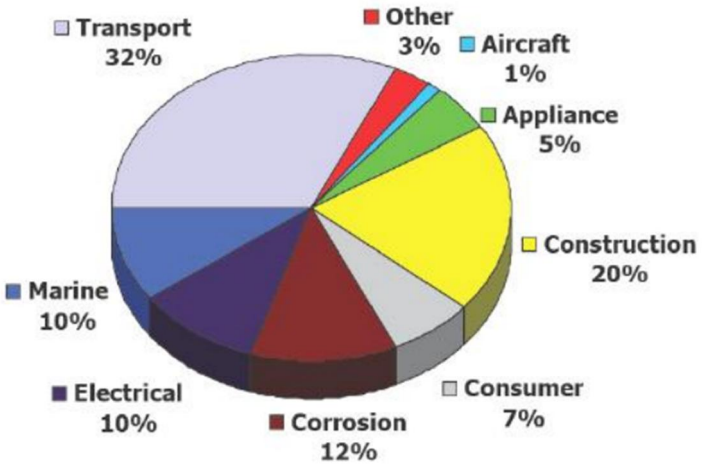

Figure 1-1: Applications of glass fiber composites

The first glass fiber was known when it was combined with a plastic polymer by Owen Corning in 1935, [3]. From that time, fiber reinforced polymers (FRP) as strong alternative materials became well-known in industry as well as in military aircraft because of their lightweight and better mechanical properties [3]. Nowadays, Fiber-reinforced composites materials were used in aircrafts, automotive, shipbuilding and several industries have been growing (Figure 1-1), because of their better mechanical properties, higher fracture toughness and Young's modulus than other materials [4-6], and they also exhibit the desirable characteristics including low density, high specific strength, high specific modulus, high corrosion resistance, and low cost [7]. Michael F. Ashby has listed the evolution until 2020

(Figure 1-2) for the selection in mechanical design [8]. It is a convenient guide for designing the procedure of composite structure, as well as very helpful to explain the role of composite materials in the future material world.

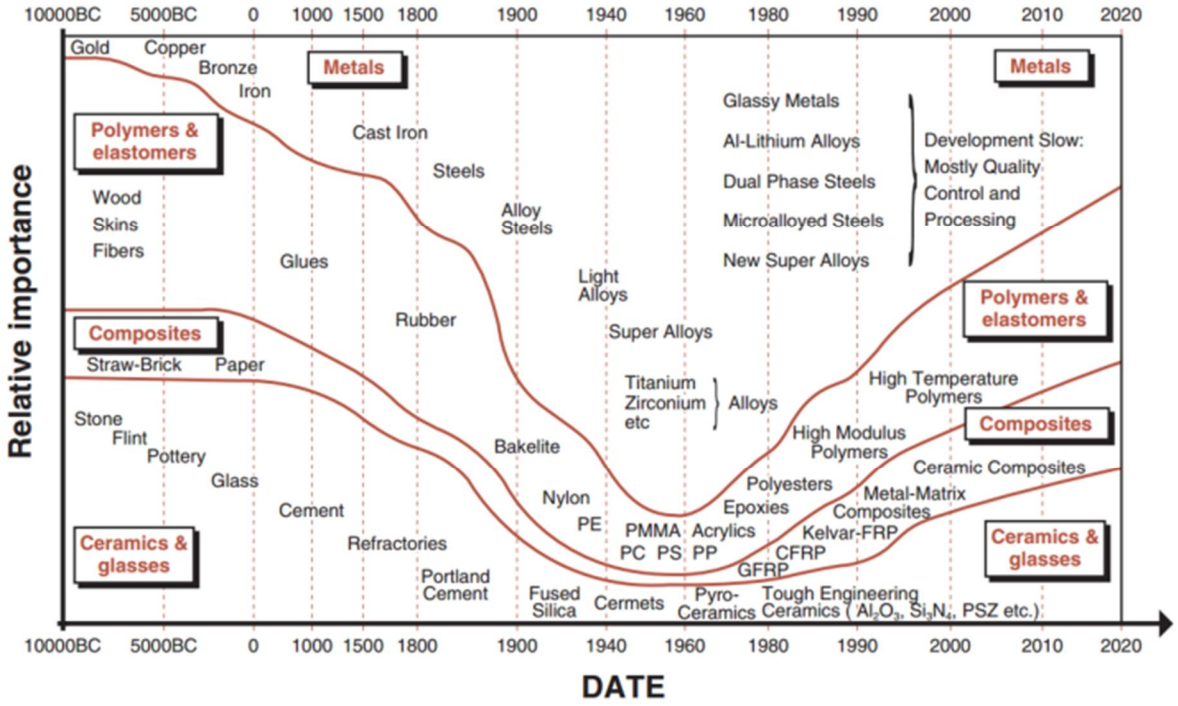

Figure 1-2: Evolution of engineering materials until 2020

1.1 Materials

1.1.1 Unsaturated polyester resin (UPR)

Polyester molecules are the cross-linkers and reactive diluents work as agent to link the adjacent polyester molecules. The curing behavior is the specific characteristic of UPR, that was presented deeply in the reference [9] as follows: The curing reaction of UPR is a free radical chain growth cross-linking polymerization between the reactive diluents (styrene monomers) and unsaturated resin. At the room temperature, methyl ethyl ketone peroxide (MEKP) is used as a hardener for the UPR curing process.

Figure 1-3: Unsaturated polyester resin (UPR)

The commercial UPR shown in Figure 1-3, with the density around 1.15g/cm^3, and MEKP, both were made by Aekyung Chemical Company (Chung nam, South Korea).

After injection of MEKP into UPR and quickly mixing evenly, the curing process will start and leads to volumetric shrinkage. The initiator decomposes to form free radicals initiating polymerization which link adjacent unsaturated resin chains through connecting styrene monomers by both inter- and intra-molecular reactions (three-dimensional networks). As the polymerization continues, the temperature and degree of polymerization increases causes shrinkage.

1.1.2 Glass fibers

There are many types of artificial synthesis fibers in the world of fiber reinforcement composites, such as glass fibers, carbon fibers, kevlar fibers and so on [9], which maybe continuous or discontinuous. Continuous-fiber composites normally have a preferred orientation, while discontinuous fibers generally have a random orientation. Examples of continuous reinforcements include unidirectional, woven cloth, and helical winding, while examples of discontinuous reinforcements are chopped fibers and random mat. The type and

quantity of the reinforcement determine the final properties (Figure 1-4).

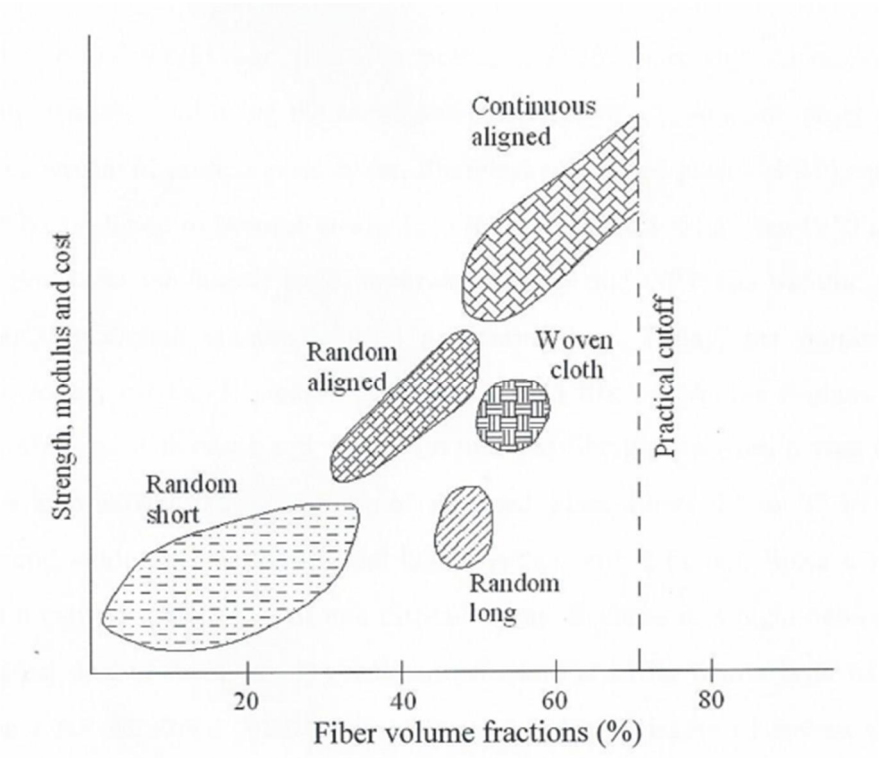

Figure 1-4: Influence of reinforcement type and quantity on composite properties

The commercial glass fibers include chopped strand mat (CSM) and woven (roving) were shown in Figure 1-5, both of them were purchased from Kimchon plant company in South Korea.

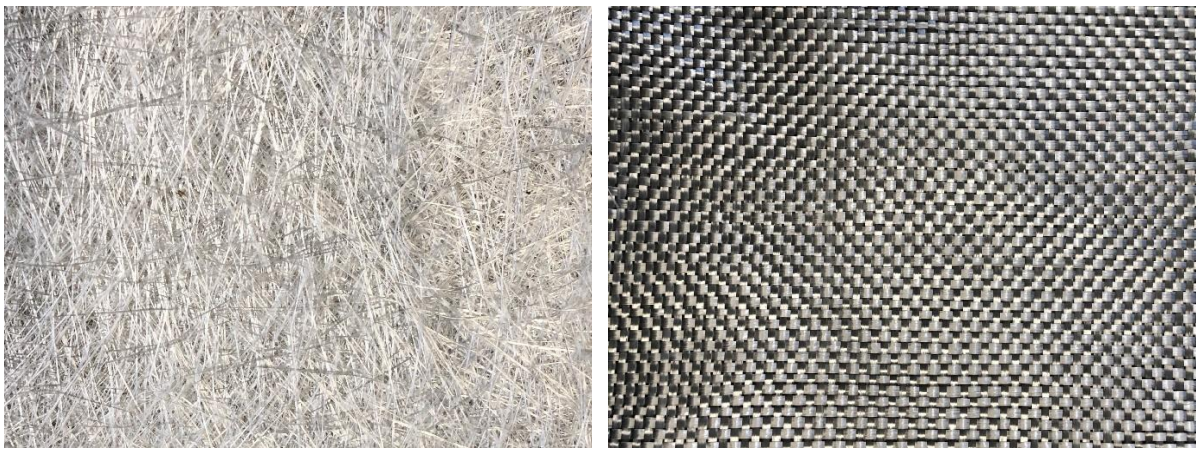

Figure 1-5: Chopped strand mat (left) and woven roving (right)

1.1.3 Multi-walled carbon nanotubes (MWCNTs)

The carbon nanotubes were discovered by Iijima [10] in 1991, then the single-walled carbon nanotubes, double-walled carbon nanotubes and multi-walled carbon nanotubes were gradually known because of their outstanding electronic, physical, and mechanical properties as time goes by. As of now, carbon fiber has been extensively studied and possesses high specific tensile strength and modulus, as well as moderate conductivity [11], which originates from the highly ordered hexagonal carbon structure with low defect density [12].

Figure 1-6 shows The MWCNTs (CM-130) with an outside diameter of 10-15 nm, an inside diameter of 5-10 nm, and length of 10-30 μm supplied by Hanwha Chemical Company in South Korea.

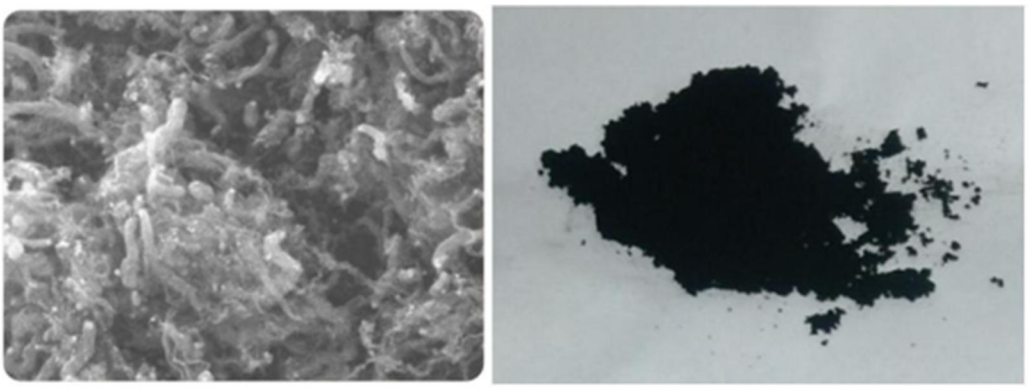

Figure 1-6: Multi-walled carbon nanotubes (CM-130)

1.2 Objectives and contents of dissertation

1.2.1 Objectives of dissertation

The effort in this dissertation aims to obtain the best combination sequence of CSM and woven reinforced composites, based on the tensile properties and interlaminar fracture toughness from mode I and mode II test. Then, the performance of same stacking sequence will be investigated under the vacuum assistant fabrication condition, mixing MWCNTs into

UPR condition as well as these two fabrication methods combining together, the fracture toughness will be obtained according to the same procedure in the previous calculation. The effect of vacuum assistant and MWCNTs will be checked by comparison with our previous study. Finally, analysis of all the stacking sequence and fabrication conditions influence will recommend the suitable stacking sequence for each fabricate condition for the future industrial production.

1.2.2 Thesis outline

In Chapter 2, the optimum stacking sequence and fabrication condition were investigated based on the density and tensile properties of composites.

The same stacking sequence and fabrication condition were used again in Chapter 3 to perform fracture test to analyze the interlaminar fracture toughness results and get the optimum conditions for industry application.

Chapter 4 summarizes the result of whole dissertation and plan of future works.

CHAPTER 2:

The effect of stacking sequence and fabrication condition on mechanical properties of various glass fibers/ unsaturated polyester resin composites

2.1 Introduction

Polymer composites have been widely used in many engineering fields due to their reliable properties, including high modulus and strength, low creep and good elevated temperature performance. Among them, glass fiber reinforced thermosetting resin is a common material because of its desirable characteristics, such as high specific strength and modulus in aerospace, automotive, shipbuilding and several industries [4-6].

For the better performance of these composites, the enhancement of composite matrix is an effective method. Many researchers added MWCNTs into the UPR to enhance the matrix property. After a well dispersion of MWCNTs in UPR pre-dispersed in tetrahydrofuran solvent with ultrasonication, the tensile strength, tensile modulus, impact strength and elongation-at-break of the nanocomposite were increased [13]. The different weight ratios of MWCNTs showed strongly positive influence on tensile and flexural strengths [14,15], and the fracture strain of composites was also enhanced [15]. The tensile strength of composites was decreased while the MWCNTs ratios increased [14-17], which means there is a certain ratio yielding the highest tensile strength values. The best weight ratio of MWCNTs mixing with UPR was investigated by stirrer method [17].

As can be seen from the current literature, most studies focus on epoxy resin and carbon fiber. Even though UPR, CSM and woven are also well-known in composites area, not any paper related to the effect of combination sequence of CSM and woven on their tensile properties under the vacuum assistant condition, MWCNTs modified UPR and these two conditions combined together. From our previous investigation [18], the fiber changes had a strong influence on tensile properties of composite structure, and the vacuum assistant had a positive tendency on the density, decomposition and tensile strength of composites. Therefore, this chapter aims to obtain higher mechanical properties of glass fibers/ unsaturated polyester

resin composites based on the suitable stacking sequence and fabrication condition.

2.2 Experiment

2.2.1 Materials

The reinforcement components are glass fiber chopped strand mat (300 g/m^2 density) and woven (570 g/m^2 density), both of them were made by Kimchon Plant Company (Seoul, South Korea).

The unsaturated polyester resin (EC-304), whose density is around 1.15g/cm^3, and methyl ethyl ketone peroxide (MEKP), both were made by Aekyung Chemical Company (Chung nam, South Korea).

The MWCNTs (CM-130) with an outside diameter of 10-15 nm, an inside diameter of 5-10 nm, and length of 10-30 μm were supplied by Hanwha Chemical Company (Ulsan, South Korea).

2.2.2 Composite structure fabrication

2.2.2.1 Matrix modification

In this study, MWCNTs were mixed with UPR by a Hotplate & Magnetic Stirrer machine (TS-17S, Jeio Tech, Seoul, South Korea) at 60℃ and 2000 rpm for 1h based on our previous results [19]. Then, the mixing temperature was reduced to the initial curing temperature range.

2.2.2.2 Composite structure fabrication

The fiber-reinforced composite was fabricated by 8 layers of fiber and matrix using the hand lay-up method. CSM and Woven layers were stacked as following different stacking sequence: $[M_4/M_4]$, $[W_4/W_4]$, $[M_4/W_4]$, $[M/W]_4$, $[M/W/M/W]_S$ and $[W/M/W/M]_S$. The same

stacking sequence was used again to fabricate under other fabrication conditions: vacuum, adding MWCNTs and applying vacuum after mixing with MWCNTs.

During the fabrication, the ratio of fiber and matrix followed Table 2-1 according to our previous results [20]. The CSM weight fraction was 0.25 and the woven weight fraction was 0.5 during the fabrication process. In the meantime, the UPR was mixed with optimum hardener ratio (1 wt.%) by hand in 30 seconds. The curing process was maintained for 24 hours after fabrication in room temperature. After curing process finished, an oven (Hanyang Scientific equipment, Seoul, South Korea) was used for post-curing at 80℃ for 2 hours since this process could remove air voids and improve crosslinking of the matrix and fiber. Finally, each plate will be cut into five specimens by diamond cutter (The University of Ulsan, Ulsan, South Korea) in a rectangular shape. The length of the specimen was 200 mm, 20 mm in width and the thickness was varied in each plate.

Table 2-1: Fiber fraction for different cases

Components		weight fraction (%)			
		CSM	Woven	MWCNTs	UPR
1	CSM + UPR	25			75
2	Woven + UPR		50		50
3	CSM + Woven + UPR	12.5	25		62.5
4	MWCNTs + UPR			0.1	100
5	CSM + MWCNTs + UPR	25		0.075	75
6	Woven + MWCNTs + UPR		50	0.1	100
7	CSM + Woven + MWCNTs + UPR	12.5	25	0.0625	62.5

In the case of using the vacuum during fabrication, a vacuum bag (Airtech, CA, USA) was used to pack composite samples, cover a bleeder (Jet Korea Aerospace Industry, Gyeoungsangnamdo, South Korea) and a peel ply (Airtech, CA, USA) on samples. After that, vacuum was maintained using a high vacuum pump (W2V10, Woosung Automa, Gyeonggido, South Korea) to assist the curing process for 5 hours.

2.2.3 Measurements

The tensile test was conducted using a universal testing machine (DTU-900MHN) at a test speed of 2 mm/min according to ASTM D3099. The center position of samples was marked after cleaning by the 200 CATALYST-C on the surface and a strain gauge (FCA-2-11-1LJB. Tokyo Sokki Kenkyujo Co., Ltd) was attached on the center of samples for measuring strain (Figure 2-1). Besides, two laser tapes were attached on the samples at the point 40 mm from the center, totally 80 mm gauge length was used for test. The tensile properties were analyzed to evaluate the effect of fabrication conditions on various composites structures.

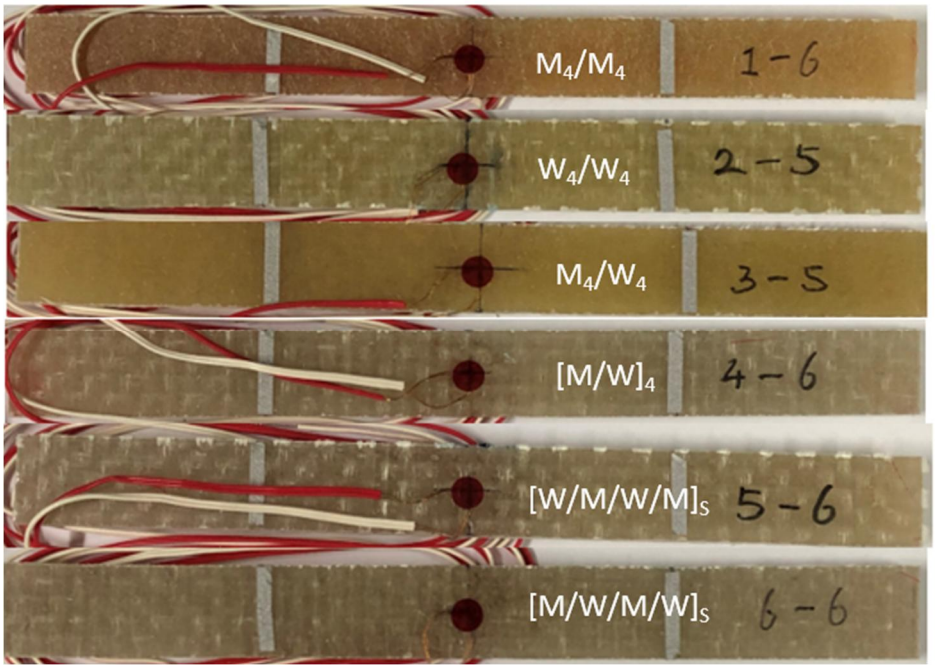

Figure 2-1: Configuration of tensile specimens

2.3 Results and discussion

2.3.1 Density of composite structure

A vacuum pump was used for post-curing process after hand lay-up fabrication, which has been known as a hybrid fabrication method [21]. Vacuum was useful to remove the unnecessary resin from samples to the cover layers such as bleeder and peel ply, even to the vacuum hoses in sometimes during experiment. The effect of vacuum was decided by the polymerization process of materials. If the process time was too short, then applying vacuum will not have too much influence for the material properties.

Table 2-2: Mass of composites in different stacking sequence

Mass (g)		UPR	UPR + Vacuum	UPR + MWCNTs	UPR+ Vacuum + MWCNTs
1	M_4/M_4	31.54	20.25	32.14	20.61
2	W_4/W_4	30.37	23.71	31.1	29.05
3	M_4/W_4	31.35	23.01	31.62	29.74
4	$[M/W]_4$	29.71	23.61	30.97	27.45
5	$[W/M/W/M]_S$	33.27	22.02	33.64	25.35
6	$[M/W/M/W]_S$	33.51	22.07	33.65	22.82

As shown in Table 2-2, after applying vacuum for the same stacking sequence, the mass was reduced obviously. Each case of composites had a small value of mass and the lightest sample was $[M_4/M_4]$ after applying vacuum, only 20.25g (decreased 35.79%). The others were: $[W_4/W_4]$ (23.71g, decreased 21.93%), $[M_4/W_4]$ (23.01g, decreased 26.61%), $[M/W]_4$ (23.61g, decreased 20.53%), $[W/M/W/M]_S$ (22.02g, decreased 33.81%) and $[M/W/M/W]_S$ (22.07g, decreased 34.14%).

Comparing the UPR + MWCNTs and the UPR + Vacuum + MWCNTs fabrication conditions, the similar result was drawn with the previous two groups. After applying the

vacuum, all the samples reached lighter mass. The mass decreased 35.87%, 6.59%, 5.95%, 11.37%, 24.64% and 32.18% in $[M_4/M_4]$, $[W_4/W_4]$, $[M_4/W_4]$, $[M/W]_4$, $[W/M/W/M]_S$ and $[M/W/M/W]_S$, respectively.

From these results, it was very obvious that the vacuum had a positive effect to reduce the mass of composites structure, but the MWCNTs did not show a similar influence on the composites' mass. The reason of this result was that the vacuum could remove extra resin from the composite plates during the curing process. For future fabrication, the vacuum assistant will be an effective method to get lighter products.

Table 2-3: Density of composites in different stacking sequence

Density (g/cm^3)		UPR	UPR + Vacuum	UPR + MWCNTs	UPR+ Vacuum + MWCNTs
1	M_4/M_4	1.4	1.54	1.38	1.53
2	W_4/W_4	1.75	1.83	1.64	1.68
3	M_4/W_4	1.57	1.68	1.54	1.6
4	$[M/W]_4$	1.56	1.69	1.52	1.59
5	$[W/M/W/M]_S$	1.5	1.7	1.49	1.64
6	$[M/W/M/W]_S$	1.51	1.73	1.5	1.66

Table 2-3 is the density of composites in different stacking sequence, where the density results also had a similar tendency with the mass of composites. For only considering the MWCNTs effect, the density was almost same for the same stacking sequence, which means it's not a good choice to improve the density of composites or get lighter parts in the same fabrication condition. But for the vacuum effect in UPR and UPR + Vacuum these two conditions, the density of composites were increased after applying vacuum. The density of $[M_4/M_4]$, $[W_4/W_4]$, $[M_4/W_4]$, $[M/W]_4$, $[W/M/W/M]_S$ and $[M/W/M/W]_S$ were increased 10%, 4.5%, 7.1%, 8.33%, 13.3% and 14.57%, respectively. Analogous results were also shown in the UPR + MWCNTs and the UPR + Vacuum + MWCNTs these two fabricate conditions,

after adding the MWCNTs into the UPR, where the density of composites using a vacuum were increased to a higher value than without the vacuum assistant, The density increased 10.87%, 2.44%, 3.89%, 4.61%, 10.07% and 10.67% in $[M_4/M_4]$, $[W_4/W_4]$, $[M_4/W_4]$, $[M/W]_4$, $[W/M/W/M]_S$ and $[M/W/M/W]_S$, respectively. Therefore, the density increase of composites may be attributed to the removing of a significant amount of UPR.

2.3.2 Tensile properties of composite structure

Table 2-4 shows the ultimate tensile strength for each case of composite plates where the vacuum assistant showed a good effect on tensile strength and MWCNTs had a strongly impact on that. By comparing with only UPR fabrication, the UPR + Vacuum + MWCNTs fabrication condition had the highest tensile strength, and the MWCNTs had a stronger effect on tensile strength than vacuum assistant of composite plates. The $[W_4/W_4]$ under vacuum & MWCNTs combined condition had the highest tensile strength (356.2 MPa).

For these three fabrication conditions, the tensile strength of $[M_4/M_4]$ increased 27.94%, 139.55% and 152.63% under vacuum assistant, MWCNTs and vacuum & MWCNTs combined conditions, respectively. The other stacking sequences: $[W_4/W_4]$ (23.45%, 40.86%, 106.36%), $[M_4/W_4]$ (9.03%, 17.23%, 101.52%), $[M/W]_4$ (31.08%, 36.81%, 136.4%), $[W/M/W/M]_S$ (48.89%, 62.79%, 160.13%) and $[M/W/M/W]_S$ (29.89%, 137.89%, 154.55%).

Table 2-4: Ultimate tensile strength in different stacking sequence (MPa)

Stress (MPa)		UPR	UPR + Vacuum	UPR + MWCNTs	UPR+ Vacuum + MWCNTs
1	M_4/M_4	72.34	92.55	173.29	182.75
2	W_4/W_4	172.61	213.08	243.14	356.20
3	M_4/W_4	120.00	130.84	140.68	241.82
4	$[M/W]_4$	120.88	158.45	165.38	257.28
5	$[W/M/W/M]_S$	127.02	189.11	206.78	330.42
6	$[M/W/M/W]_S$	90.72	117.84	215.81	230.93

When the fibers only combine with UPR fabrication condition, the [W_4/W_4] combination had the highest Young's modulus (16.49 GPa) in 6 stacking sequences (Figure 2-2 (a)), and [M_4/M_4] showed the lowest value (8.03 GPa). Other stacking sequences show medium value, and the order is as follows: $[W/M/W/M]_S$ (14.8 GPa), $[M/W]_4$ (12.84 GPa), [M_4/W_4] (12.25 GPa) , $[M/W/M/W]_S$ (10.44 GPa). The reason for this order is the fiber length and structure were different, Woven had longer fiber length and orthogonal braided structure, while CSM had the random directions and the short length of fiber. The longer fiber reinforced composites showed higher viscoelastic properties, Young's modulus, and melting temperature but showed less uniform distribution of fibers [19].

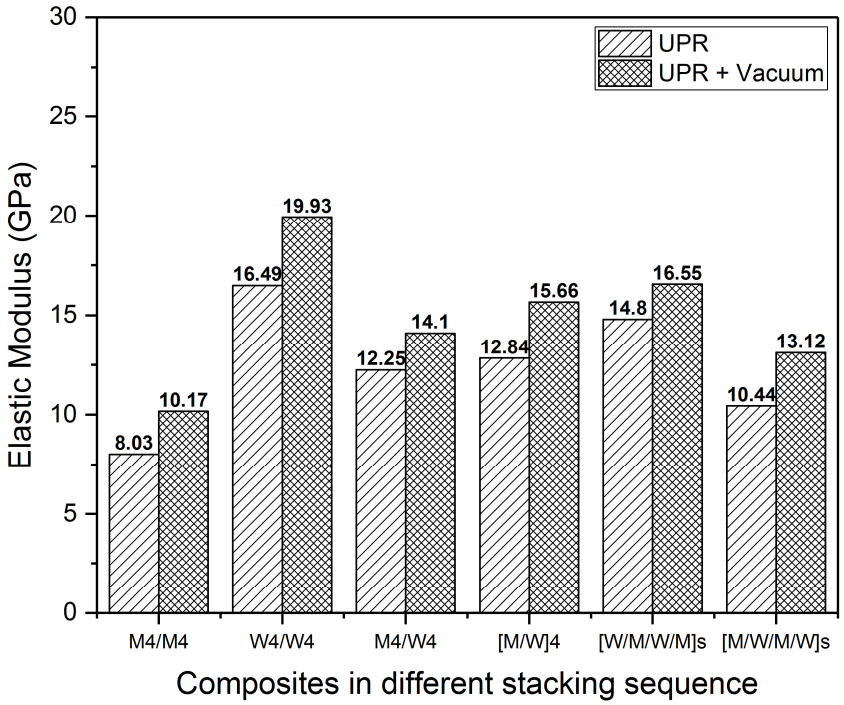

(a) Vacuum effect on Young's modulus

For the same stacking sequences under vacuum assistance during the experiment, the Young's modulus values for samples were increased to varying degrees shown in Figure 2-2 (a). [W_4/W_4] had the highest value 19.93 GPa (increased 20.86%), the Young's modulus of other stacking sequences as follows: $[W/M/W/M]_S$ 16.55 GPa (increased 11.82%) , $[M/W]_4$

15.66 GPa (increased 21.96%), [M_4/W_4] 14.1 GPa (increased 15.1%), [M/W/M/W]$_S$ 13.12 GPa (increased 25.67%), [M_4/M_4] 10.17 GPa (increased 26.65%). It means that the vacuum has a positive effect on the elastic modulus of fiber-reinforced composites. Considering the elastic modulus of samples under the vacuum effect, the stacking sequence [W_4/W_4] was recommended.

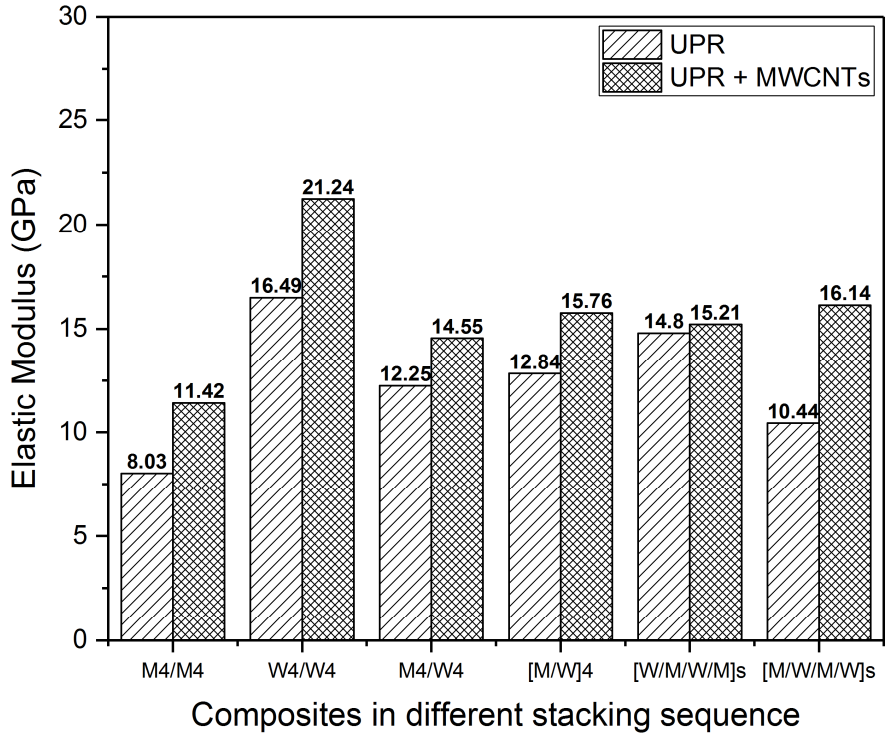

(b) MWCNTs effect on Young's modulus

Fig 2-2 (b) showed the MWCNTs effects on the elastic modulus of samples, where MWCNTs had a positive influence on the Young's modulus among all the stacking sequences. The [W_4/W_4] combination had the best performance in all the stacking sequences. The Young's modulus increased from 16.49 GPa to 21.24 GPa (28.81%), The Young's modulus of [M/W/M/W]$_S$, [M/W]$_4$, [W/M/W/M]$_S$, [M_4/W_4], [M_4/M_4] increased 5.7 GPa (54.59%), 2.92 GPa (22.74%), 0.41 GPa (2.77%), 2.3 GPa (18.78%) and 3.39 GPa (42.22%), respectively. The effect of MWCNTs presents the same tendency with our previous experiment conclusion [20]. Thus, for mixing MWCNTs cases, the combination of [W_4/W_4] was recommended

among all the stacking sequences based on higher Young's modulus.

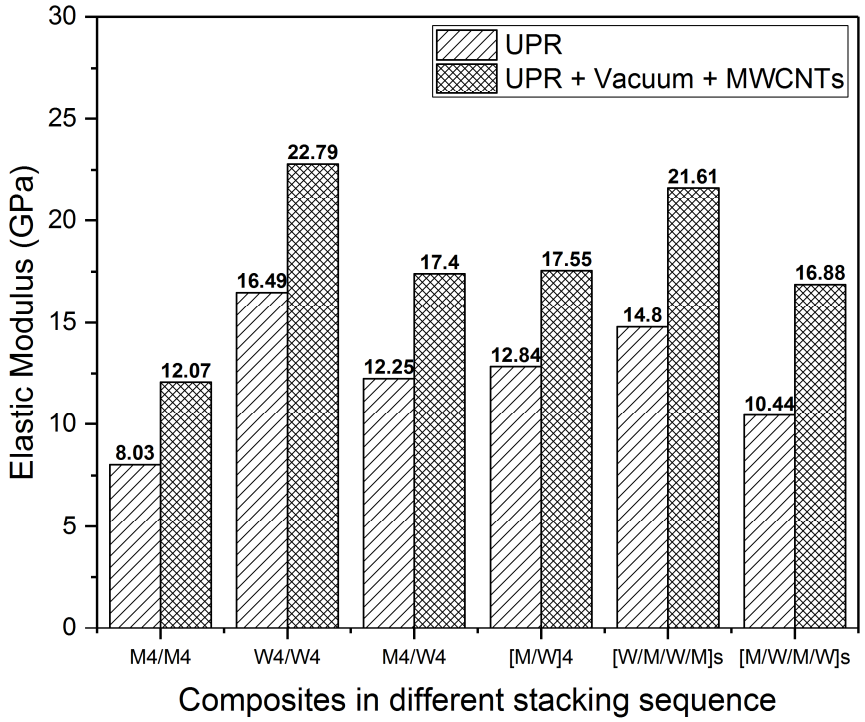

(c) Vacuum & MWCNTs effect on Young's modulus

Figure 2-2: Young's modulus of composites

As can be seen from Fig 2-2 (c), Vacuum & MWCNTs combinations have a strong effect on the Young's modulus for each stacking sequence and present a better performance than only vacuum or MWCNTs effect. The combination of $[W_4/W_4]$ (22.79 GPa) possessed the highest value than others. $[M_4/M_4]$ showed the lowest Young's modulus in all stacking sequence (12.07 GPa). Each of the samples has achieved significantly higher Young's modulus. Order of others is as follows: $[W/M/W/M]_S$ (21.61 GPa), $[M/W]_4$ (17.55 GPa), $[M_4/W_4]$ (17.4 GPa), $[M/W/M/W]_S$ (16.88 GPa). Under the vacuum & MWCNTs combined fabrication condition, the $[W_4/W_4]$ combination was recommended because of the higher Young's modulus.

Table 2-5 shows the Poisson's ratio of composites in different stacking sequence. Poisson's ratio of each composites was measured by the strain gauge and recorded by the

STRAINSMART software automatically. As one of the basic factors of material properties, it will be used for the future finite element analysis to check the simulation results.

Table 2-5: Poisson's ratios of composites in different stacking sequence

Poisson's ratio		UPR	UPR + Vacuum	UPR + MWCNTs	UPR+ Vacuum + MWCNTs
1	M_4/M_4	0.35	0.43	0.34	0.38
2	W_4/W_4	0.11	0.12	0.25	0.16
3	M_4/W_4	0.37	0.43	0.32	0.34
4	$[M/W]_4$	0.17	0.19	0.23	0.17
5	$[W/M/W/M]_S$	0.2	0.24	0.22	0.25
6	$[M/W/M/W]_S$	0.19	0.23	0.21	0.24

From above results, when mat or woven was used only to fabricate composite plates, we could observe woven had a better tensile property (higher tensile strength and Young's modulus) than mat because woven had a long fiber and orthogonal structure. The chopped strand mat showed great potential when the matrix is added by MWCNTs since chopped strand mat had random, short fibers which could combine with MWCNTs easier for one layer, and also combine with other layers more tightly. As for combining these two kinds of fibers, $[W/M/W/M]_S$ had the best performance among four stacking sequences, it proved that the composite structure had a great influence of tensile properties and the detailed reasons will be investigated in Chapter 3.

2.4 Conclusion

In this chapter, different fabrication condition was applied to investigate the effect of stacking sequence on tensile properties of various glass fiber composites. The stacking sequence strongly impacted the tensile properties of fiber-reinforced composites. Applying vacuum has a positive influence on the density, thickness, mass and tensile properties of composites. In comparison to the compression molding method, a vacuum may have less effect on the mechanical properties but it is a simple, more flexible and convenient method with a variety of product geometries. MWCNTs also possessed a good effect on the tensile properties of composite structure. Additionally, the vacuum & MWCNTs combined fabrication condition showed the best performance among all the conditions. Therefore, based on the better performance in all the factors (density, thickness, mass and tensile properties), the [W_4/W_4] combination under vacuum & MWCNTs fabrication condition was recommended temporarily. For the future application in the industry, the fracture toughness will be considered, either. After analyzing all the factors of composites, the best stacking sequences will be suggested for future products in several industrial fields.

CHAPTER 3:

The effect of fabrication condition on fracture toughness of various glass fiber composites

3.1 Introduction

There are three modes in fracture mechanics applying force to enable a crack to propagate: mode I, mode II and mode III (mix-mode) are shown in Figure 3-1.

Mode I (opening mode): a tensile stress normal to the plane of the crack.

Mode II (sliding mode): a shear stress acting parallel to the plane of the crack and perpendicular to the crack front.

Mode III (tearing mode): a shear stress acting parallel to the plane of the crack and parallel to the crack front.

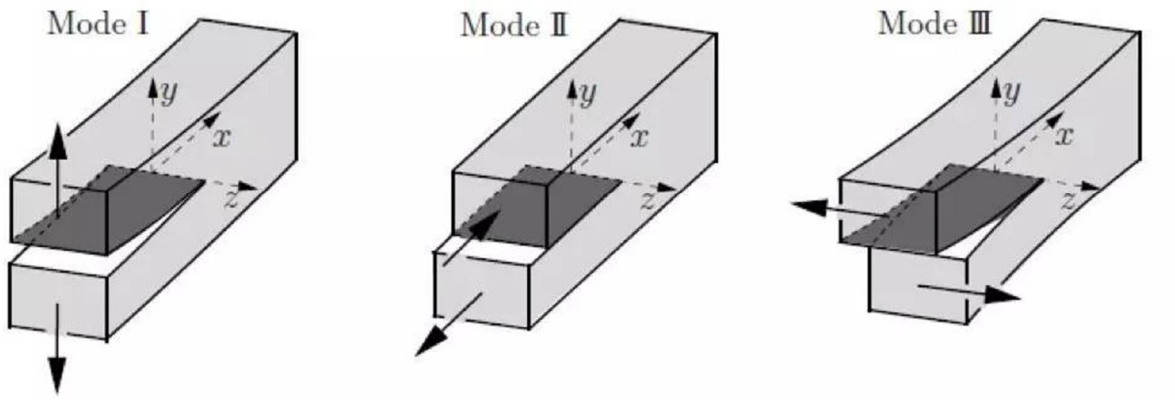

Figure 3-1: Three fracture modes

There are many types of specimen which could be used to investigate the fracture toughness, such as double cantilever beam, end-notched flexural, compact tension and so on. Fracture toughness is a quantitative indicator in mode I and mode II fracture test, the critical values of the stress intensity factor or the strain energy release rate that has been used to measure the interlaminar fracture toughness of composite materials [22,23]. The interlaminar fracture toughness has been identified as a prime factor in controlling the growth of existing delamination [24]. Surface treatments could change the level of adhesion between fibers and

matrix, thus will result in an increase of the fiber-matrix interfacial shear strength and interlaminar fracture toughness [25]. A double cantilever beam (DCB) type specimen has been utilized by a number of works [26-28] to determine mode I interlaminar fracture toughness of fiber reinforced composite materials. The carbon nanotubes modified laminates so that they could exhibit higher mode II interlaminar fracture toughness value and interlaminar shear strength than the base laminates [29]. Several results focused on fracture toughness of the unidirectional fiber composites [30-34], and several of them considered CSM or Woven separately [35,36]. However, there are not many papers considering the combination of both materials and their stacking sequence effect on fracture toughness. The stacking sequence is also an influential factor of composites which affected the impact resistance [37], the maximum strength [38] and the energy release rate distributions [39]. Only a few papers considered the effect of stacking sequence on fracture toughness.

As can be seen from the current literature, most studies focus on epoxy resin and carbon fiber. There are a few papers which consider the effect of combination sequence of CSM and woven on their fracture toughness under the vacuum assistant condition, MWCNTs modified UPR and these two conditions combined together. From our previous investigation [20], the fiber changes had a strong influence on tensile properties of composite structure, and the vacuum assistant had a positive tendency on the density, decomposition and tensile strength of composites. Motivated by the above conclusions, this chapter aims to obtain the best combination sequence of CSM and woven reinforced composites based on the interlaminar fracture toughness from mode I and mode II test first. Secondly, the performance of same stacking sequences was investigated under the vacuum assistant fabrication condition, mixing MWCNTs into UPR condition as well as these two fabrication methods combining together, thus obtained the fracture toughness according to the same procedure in the previous calculation. The effect of vacuum assistant and MWCNTs were checked by comparison with

our previous study. Finally, analysis of all the stacking sequence and fabrication conditions influence will recommend the suitable stacking sequence for each fabrication condition in the future industrial production.

3.2 Experiment

3.2.1 Materials

The reinforcement components are glass fiber chopped strand mat (300 g/m^2 density) and woven (570 g/m^2 density), both of them were made by Kimchon Plant Company (Seoul, South Korea).

The unsaturated polyester resin (EC-304), whose density is around 1.15g/cm^3, and methyl ethyl ketone peroxide (MEKP), both were made by Aekyung Chemical Company (Chung nam, South Korea).

The MWCNTs (CM-130) with an outside diameter of 10-15 nm, an inside diameter of 5-10 nm, and length of 10-30 μm were supplied by Hanwha Chemical Company (Ulsan, South Korea).

3.2.2 Composite structure fabrication

The composites plates were fabricated by 8 layers of different glass fibers reinforced UPR using the hand lay-up method. CSM and Woven layers were stacked as the same sequences as Chapter 2, as well as the same fabrication conditions were used. During the fabrication, the initial crack was created by inserting a 25 μm thickness Teflon film in the mid-plane of all plates. The size of composites plates were 220 mm in length and 240 in width. The weight fraction of CSM and woven were 25% and 50% in composite fabrication, which were already illustrated in Table 2-1. Besides, the UPR was mixed with hardener (optimum ratio 1 wt.%)

by hand in 30 seconds.

The curing process was maintained for 24 hours after fabrication in room temperature. After the curing process finished, the plates were kept in an oven at 80℃ for 2 hours for post-curing. Then, the plates will be cut by a diamond cutter in a rectangular shape. The DCB (Double cantilever beam) and ENF (End-notched flexural) samples with the same parameters were obtained (200 mm in length and 20 mm in width), while the thickness varied with different samples (Figure 3-2).

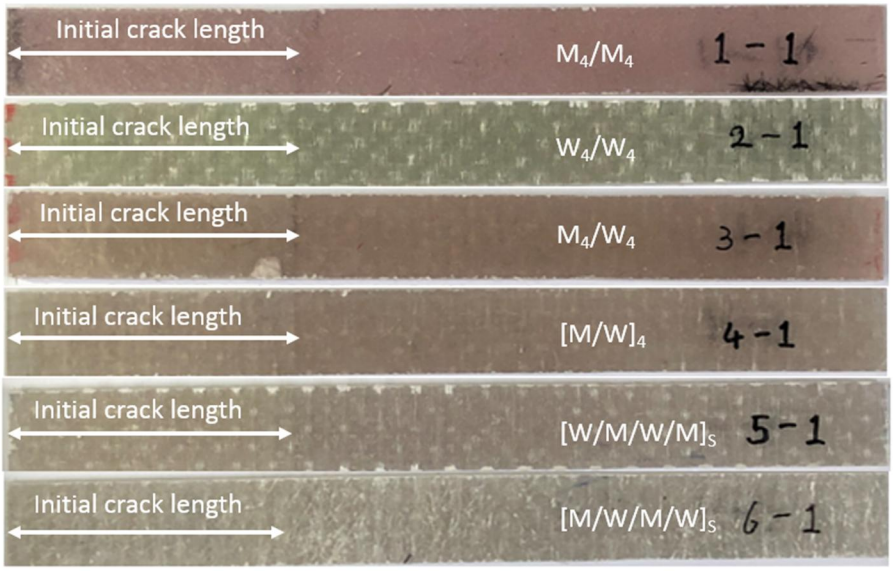

Figure 3-2: Configuration of mode I and mode II specimens

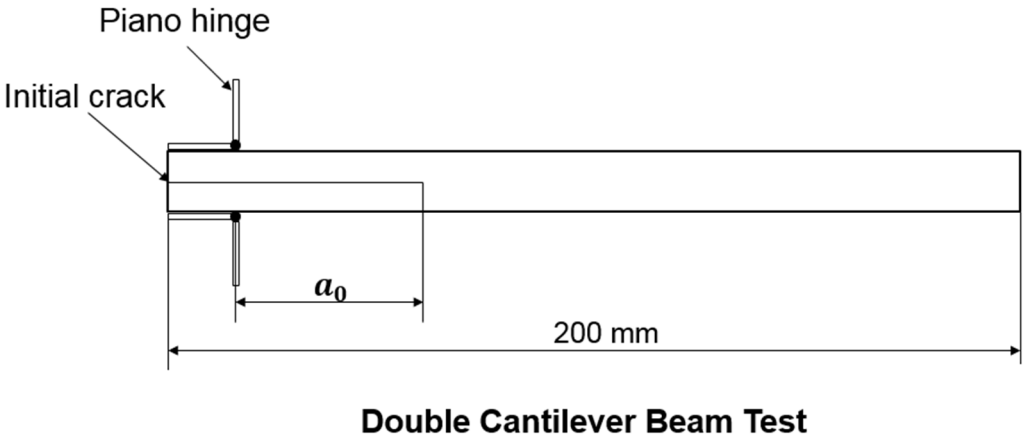

Figure 3-3: Dimensions of DCB specimen

According to ASTM D5528-3, piano hinges will be attached at the edges of DCB samples. Both of the hinges and samples attachment area were smoothed by rough sandpaper, and then cleaned by acetone before using rabbit bond to attach them together. What's more, DCB samples were marked at the crack tip position and crack propagation length with every 5 mm interval for 10 positions. The dimensions of DCB specimen were given in Figure 3-3.

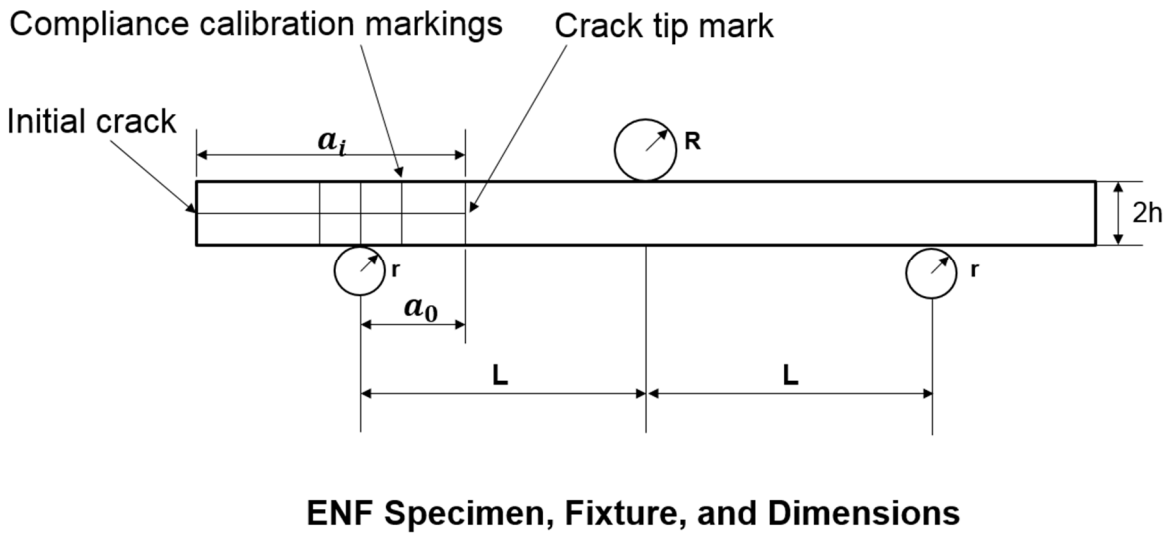

Figure 3-4: Dimensions of ENF specimen and experimental set-up

Non-Precracked (NPC) method was used for ENF specimens which followed ASTM D7905/D7905M-14, 3 crack lengths (20 mm, 30 mm and 40 mm from the crack end) were marked for applied loading. NPC toughness means the interlaminar fracture toughness value which was determined from the pre-implanted insert. The dimensions of ENF specimen were given in Figure 3-4.

3.2.3 Testing

DCB specimens were tested by a tension loading at 2.4 mm/min test speed, the crack propagation was visually recorded by naked-eyes and stopwatch timer while matching with load and displacement by time. ENF samples were tested by 3 points bending method at 0.8 mm/min test speed and the span length was fixed in 100 mm. All of the tests were performed

by EUN SUNG universal testing machine (Figure 3-5) and the load and displacement data were recorded by DT board (DAQ DT9839) at a frequency of 200 Hz.

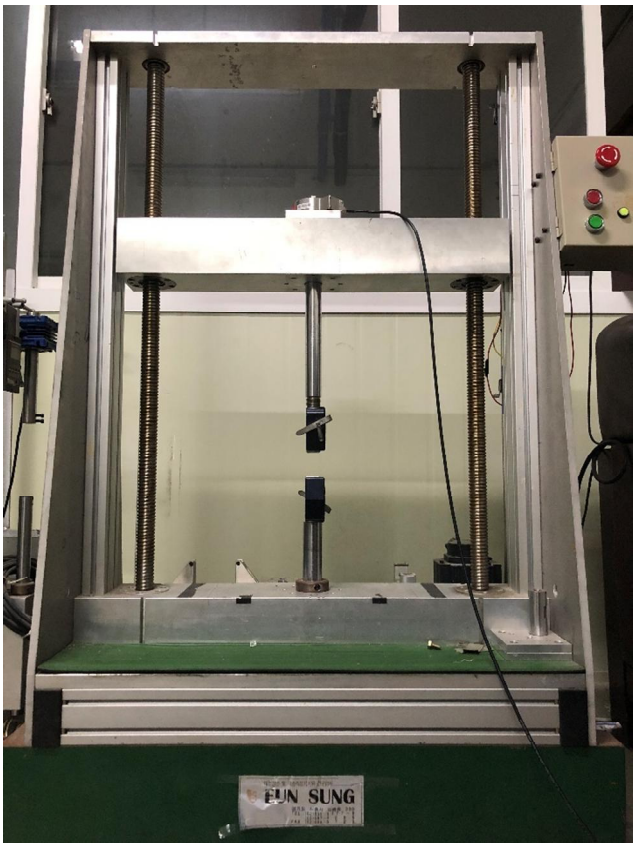

Figure 3-5: Configuration of fracture testing machine

3.3 Calculations

3.3.1 Double Cantilever Beam (DCB) test

On the DCB samples, 10 positions were marked at every 5mm from the crack tip which is denoted by a_0, up to 50mm as crack propagation length for later calculation. Modified beam theory method was used to calculate the interlaminar fracture toughness according to ASTM 5528 [40] and the equation is as follows:

$$G_I = \frac{3P\delta}{2b(a+|\Delta|)} \tag{3-1}$$

Here:

- G_I = mode I interlaminar fracture toughness, kJ/m^2,

- P = load, N.

- δ = load point displacement, mm.

- b = specimen width, mm.

- a = delamination length, mm.

-Δ = correcting delamination length due to the rotation of beam during loading, mm. It can be calculated by linear relation of the cubic root of compliance $C^{1/3}$ and delamination length a. Where compliance is

$$\mathrm{C} = \delta/P \tag{3-2}$$

By using the Microsoft Excel, we can get the Δ value easily. Firstly, plot the curve of cubic root of compliance $C^{1/3}$ and delamination length a; after that, using linear regression method to fit the curve and export the function, then the accuracy of this function could be evaluated by R^2 value which should be close to $R^2 = 1$. Finally, solving the linear function and we will get Δ value.

An example is shown in Figure 3-6 for the procedure. The black curve is the true relationship of $C^{1/3}$ and a, and the red one is the linear regression function. $R^2 = 0.998$ means the fitting curve is reasonable, thus we can calculate Δ by solving the equation: 0.0144x-0.0326=0, then x=2.26, which means $\Delta = 2.26$.

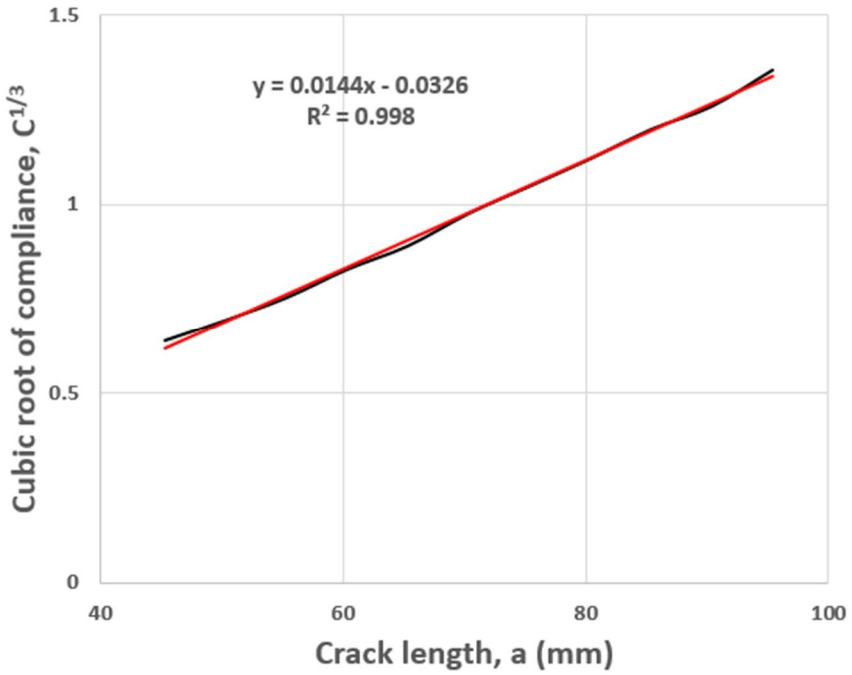

Figure 3-6: Determination of correcting delamination length

3.3.2 End-notched flexure (ENF) test

On the ENF samples, 3 crack length values were marked at 20mm, 30mm and 40mm from the crack tip. The first compliance calibration (CC) test was performed at crack length equal to 20 mm with 50% of critical load and the specimen was then repositioned at a=40mm with 50% of critical load. Then, the non-precracked fracture test will be performed in the fixture a=30mm to get the mode II fracture toughness value.

The candidate fracture toughness of mode II is determined using the equation in ASTM 7905 [41]:

$$G_Q = \frac{3mP_{Max}^2 a_0^2}{2B} \tag{3-3}$$

where m is the compliance calibration coefficient (CC coefficient), P_{Max} is the maximum force from the fracture test, a_0 is the crack length used in the fracture test (30

mm), and B is the specimen width.

The CC coefficients, A and m, are to be determined using a linear least squares linear regression analysis of the compliance, C, versus crack length cubed data of the form:

$$C = A + ma^3 \tag{3-4}$$

Where A is the intercept and m is the slope obtained from the regression analysis.

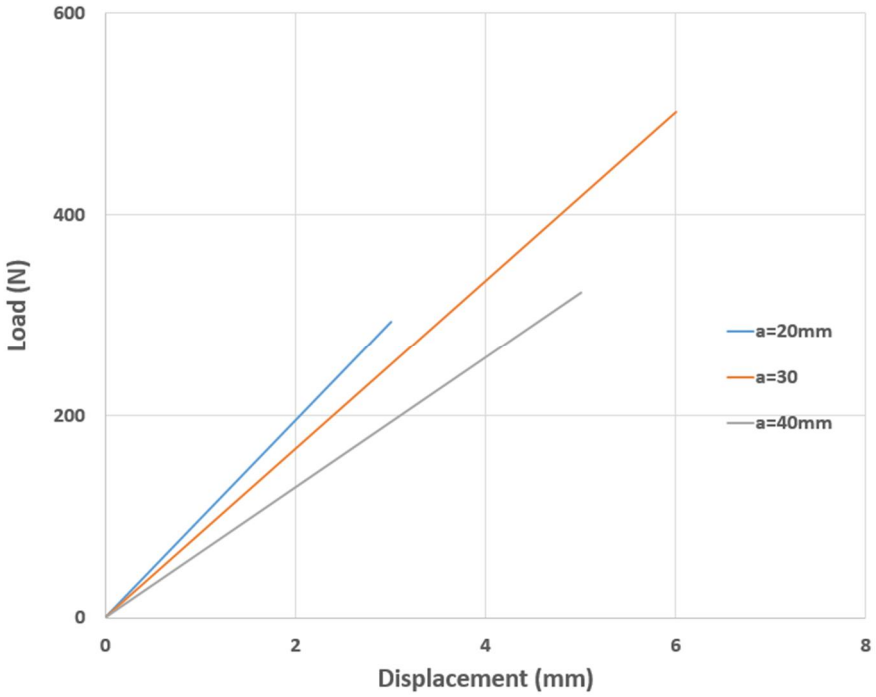

Figure 3-7: Load-Displacement relation curves of different crack length in mode II test

Load-displacement relation curves of CC test and NPC fracture test example are shown in Figure 3-7 and from these three curves' regression function, the compliance for each crack length position could be easily calculated.

The linear regression function could be found to fit the compliance and the crack length cubed in Microsoft Excel. There are only 3 values of C and a from the curve (Figure 3-8). The red line was the real relation of compliance C and crack length cubed a^3, while the black one was the linear regression function. $R^2 = 1$ means the result was matched perfectly.

Thus, according to equation (3-4), we can know for this case, $A = 0.0094$ and $m = 9 \times 10^{-8}$.

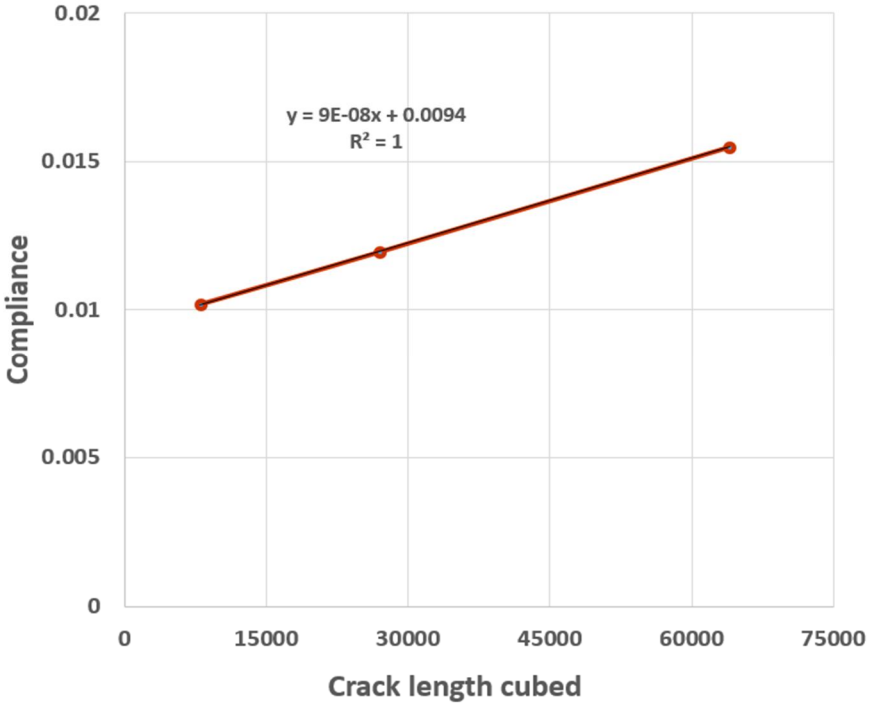

Figure 3-8: Linear regression function of compliance and delamination length cubed

The flexural modulus is calculated as follows:

$$E_{lf} = \frac{L^3}{4ABh^3} \tag{3-5}$$

Where A is the CC coefficient obtained during CC test of the specimen.

3.4 Results and discussions

3.4.1 Mode I fracture test results

Figure 3-9 shows the load-displacement curve for all the samples test by Double Cantilever Beam (DCB) test. It indicates load and displacement at first deviation from nonlinearity and at the visual onset of delamination from either edge. In addition, the compliance values could be extracted from the load-displacement curve for each specimen,

which is one parameter for calculating the interlaminar fracture toughness from Eq.1 according to ASTM 5528.

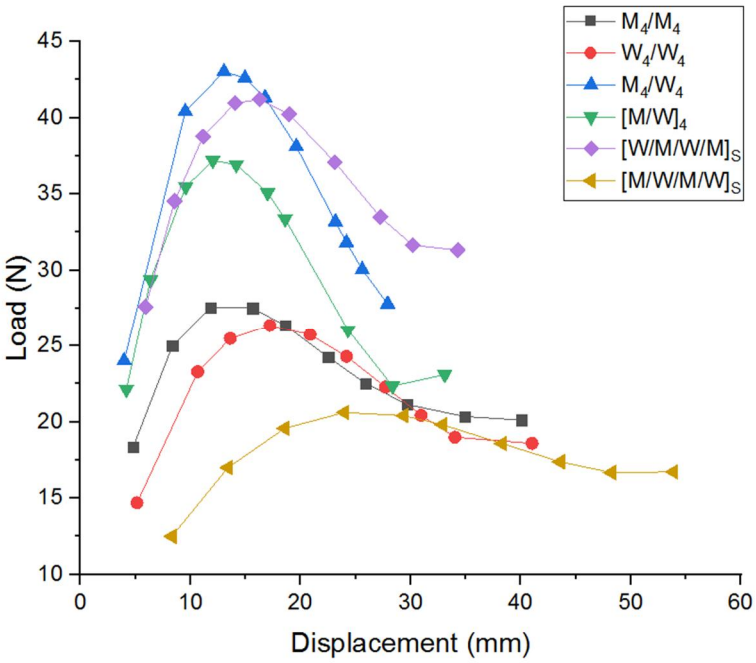

Figure 3-9: Load-Displacement relation of composite

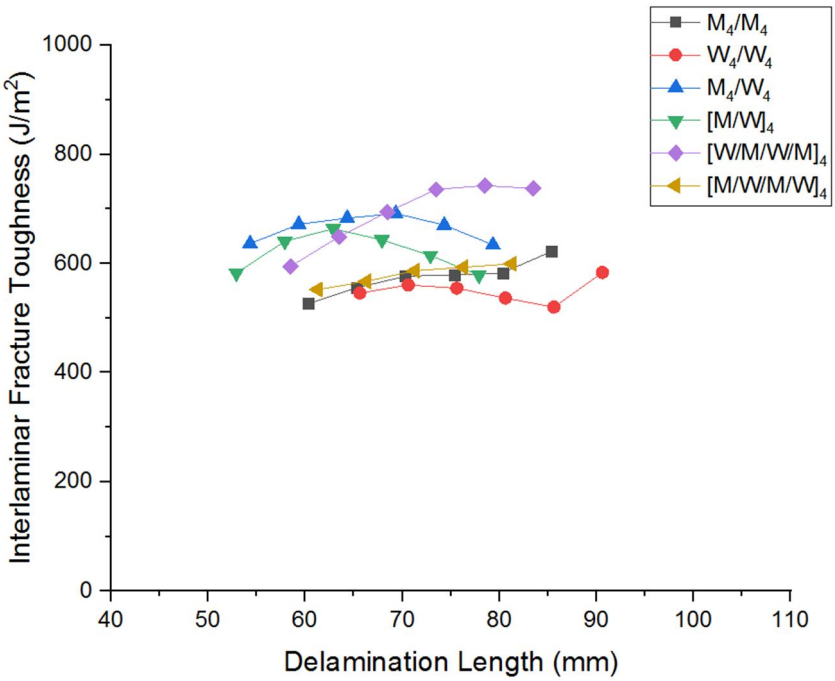

Figure 3-10: Delamination resistance curve of composites

The delamination resistance curve (Figure 3-10) was also generated by calculated values

according to ASTM. It is significantly dependent on the strength of resin, bridging fiber or interfacial strength of fiber and matrix [42]. The initial fracture toughness was very small in comparison with other crack propagation positions. In this study, longer crack length region was considered (>50mm), which is more intuitive to get better performance for different stacking sequence. The higher crack length showed more stable delamination resistance and constant values. The principal reason for the delamination resistance is fiber bridging in the center layer (Figure 3-11).

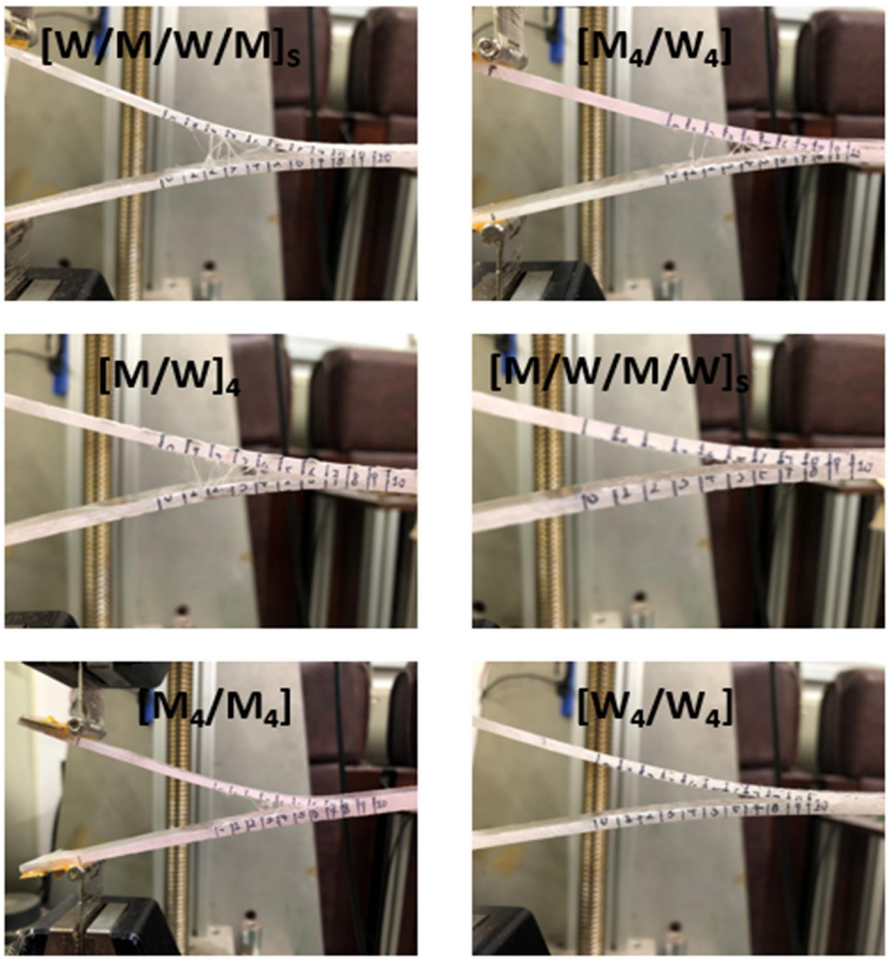

Figure 3-11: Fiber bridge in center layers of composites

After applying tensile load, the crack started to propagate along the fragile part inside the matrix (UPR). When the center layers including at least one layer of chopped strand mat, the fiber bridging will be observed easier than others. Because the fibers will not break directly, it could pull each other to resist the crack propagation, then the fiber bridging was observed.

Even for woven, it also had the fiber bridging in the center layers, but it was only some short surface fibers not the original fiber. The fibers couldn't cross layers like chopped strand mat because of its regular weave structure.

Mode I interlaminar fracture toughness for each stacking sequence in only UPR and vacuum assistant fabrication condition are shown in Figure 3-12(a). When the fibers are only combined with UPR, the $[W/M/W/M]_S$ combination shows the highest fracture toughness value in all stacking sequence (706.37 J/m^2), and $[W_4/W_4]$ combination has the lowest value (550.57 J/m^2). Other stacking sequences show medium value, and the order is as follows: $[M_4/W_4]$ (655.78 J/m^2), $[M/W]_4$ (626.23 J/m^2), $[M_4/M_4]$(573.73 J/m^2), $[M/W/M/W]_S$ (564.27 J/m^2). The reason for this order is the materials combination in center layers. Clearly fiber bridge could be observed in Figure 3-10, M/M and M/W combinations, where due to the chopped strand mat material characteristics, it is easier to produce fiber bridge than woven.

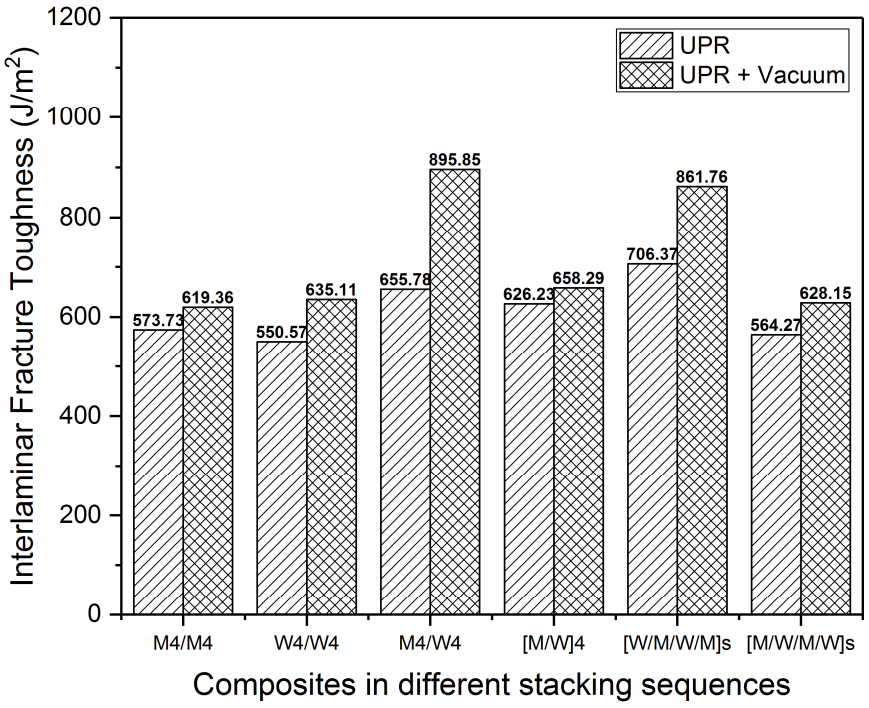

(a) Vacuum effect on mode I fracture toughness

After applying vacuum during fabrication, all samples showed higher fracture toughness

value than without vacuum assistant. The $[W/M/W/M]_S$ combination still showed the higher value (861.76 J/m^2), which means this sequence is superior to others under these two fabrication conditions. The order of fracture toughness under vacuum condition is almost the same as only UPR case, but $[M_4/W_4]$ shows great potential under the vacuum effect (36.61% increased). The rest sequences are as follows: M_4/W_4 (895.85 J/m^2), $[M/W]_4$ (658.29 J/m^2), $[W_4/W_4]$ (635.11 J/m^2), $[M/W/M/W]_S$ (628.15 J/m^2), $[M_4/M_4]$ (619.36 J/m^2). These results also matched with our previous conclusion [18], which states the vacuum assistant had a positive effect on mode I fracture toughness.

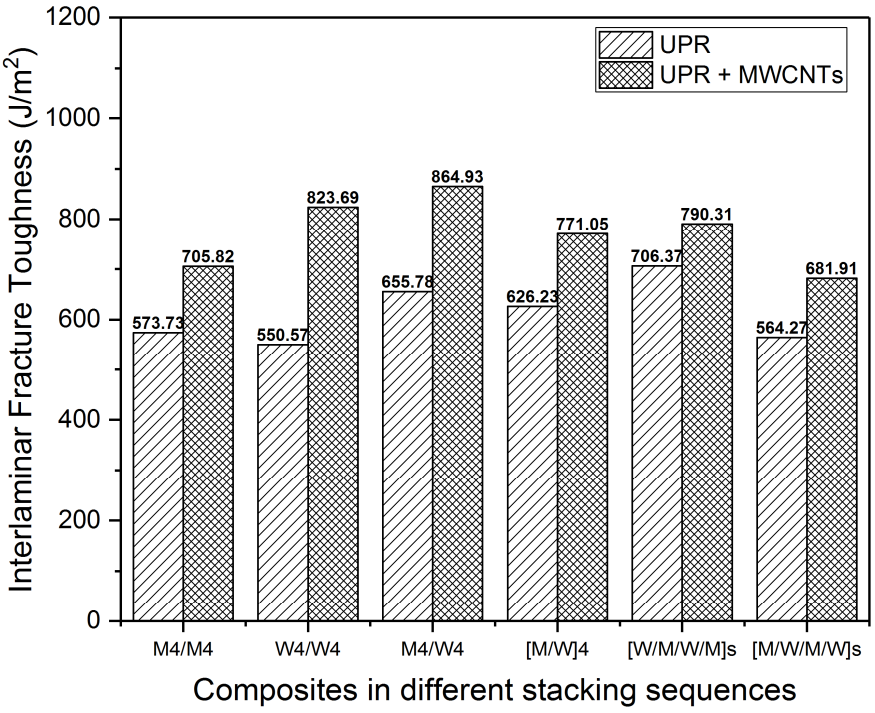

(b) MWCNTs effect on mode I fracture toughness

As can be seen from Fig 3-12(b), MWCNTs have a strong effect on the fracture toughness for each stacking sequence. The combination of $[M_4/W_4]$ (864.93 J/m^2) possessed the highest value than others. $[M/W/M/W]_S$ showed the lowest fracture toughness value in all stacking sequences (681.91 J/m^2). Because of the MWCNTs mixing with UPR, the fiber bridge in center layers got enhanced than pristine fiber, and also the matrix has better performance. The

effect of MWCNTs presents the same tendency with our previous experiment conclusion [32]. Each of the samples with MWCNTs has achieved significantly higher fracture toughness value. Order of others is as follows: $[W_4/W_4]$ (823.69 J/m^2), $[W/M/W/M]_S$ (790.31 J/m^2), $[M/W]_4$ (771.05 J/m^2), $[M_4/M_4]$ (705.82 J/m^2).

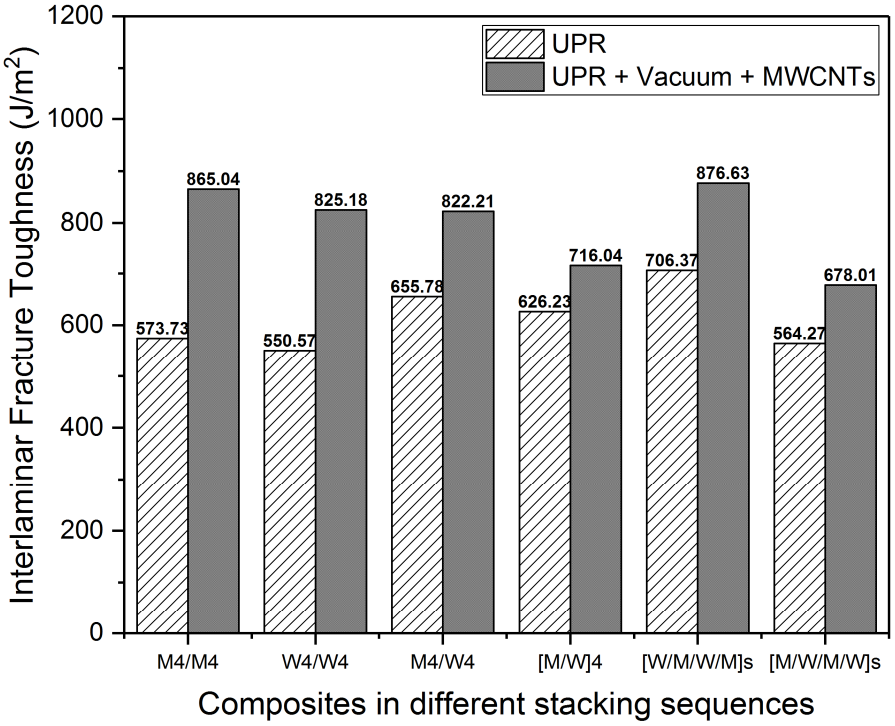

(c) Vacuum & MWCNTs effect on mode I fracture toughness

Figure 3-12: Mode I fracture toughness of composites

Figure 3-12(c) shows the fracture toughness in various stacking sequence under the vacuum assistant and MWCNTs addition. The $[M_4/M_4]$ specimen showed a great potential of fracture toughness 865.04 J/m^2 (50.77% increased). Considering the vacuum and MWCNTs effect, $[W/M/W/M]_S$ combination had the highest fracture toughness (876.63 J/m^2). $[W_4/W_4]$ (825.18 J/m^2), $[M_4/W_4]$ (822.21 J/m^2), $[M/W]_4$ (716.04 J/m^2), $[M/W/M/W]_S$ (678.01 J/m^2) increased 49.88%, 25.38%, 14.34% and 20.16% separately in fracture toughness.

In all cases of mode I fracture test, $[M_4/W_4]$ had the highest fracture toughness value under the vacuum assistant and MWCNTs addition condition. $[W/M/W/M]_S$ showed the highest

value when only combined with UPR and under vacuum & MWCNTs fabrication condition, and also presented higher values in the other two conditions. The main reason of mode I interlaminar fracture toughness was the fiber bridging in the center layers. Fiber reinforced composites can develop large scale bridging upon mode I fracture. Analyzing the bridging/toughening of short fibers in SMC plates with mode I crack, the modeling results show that the main parameters for toughening are fiber length and fiber bridge on the interface [43]. Due to the development of bridge ligaments, the fracture energy increases during crack propagation, both of bridging bundles and the toughness plays an important role in the ERR due to bridging [44]. The different fibers and their stacking sequences represented the different amount of fiber bridging which distinguishes fracture toughness values.

3.4.2 Mode II fracture test results

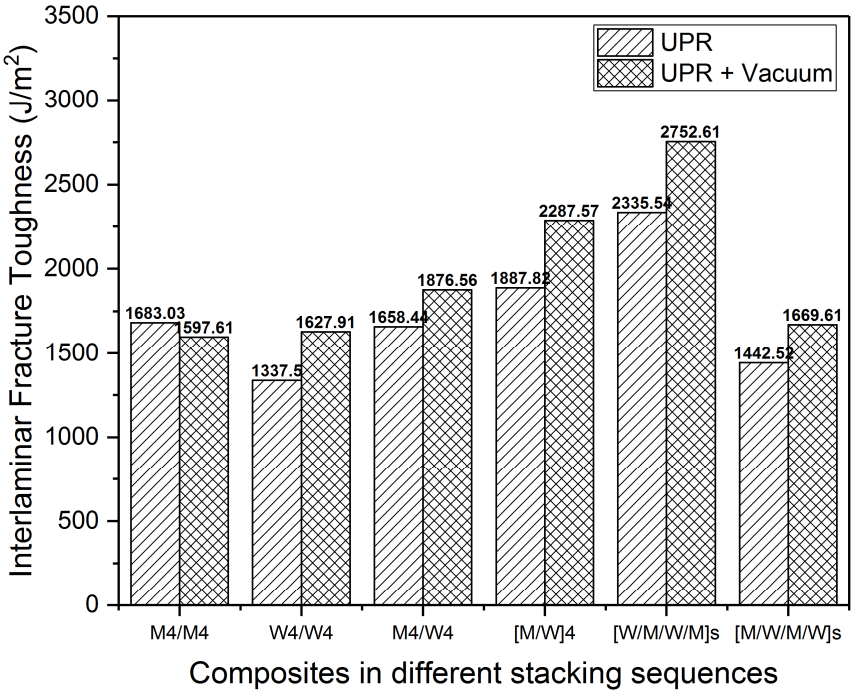

(a) Vacuum effect on mode II fracture toughness

Almost the same tendency was also achieved from mode II fracture test for various stacking sequences of composites and shown in Fig 3-13. $[W/M/W/M]_S$ combination still got

the highest toughness value without vacuum effect (2335.54 J/m^2). That means during these two kinds of fracture test, the best choice for stacking sequence was $[W/M/W/M]_S$. As can be seen in Figure 3-13(a), the order of fracture toughness for only UPR group samples were $[M/W]_4$ (1887.82 J/m^2), $[M_4/M_4]$ (1683.03 J/m^2), $[M_4/W_4]$ (1658.44.97 J/m^2), $[M/W/M/W]_S$ (1442.52 J/m^2), $[W_4/W_4]$ (1337.50 J/m^2).

For the same stacking sequences under vacuum assistance during the experiment, the fracture toughness values for samples were $[W/M/W/M]_S$ (2752.61 J/m^2), $[M/W]_4$ (2287.57 J/m^2), $[M_4/W_4]$ (1876.56 J/m^2), $[M/W/M/W]_S$ (1669.61 J/m^2), $[W_4/W_4]$ (1627.91 J/m^2), $[M_4/M_4]$ (1597.61 J/m^2), which means under the vacuum effect and without vacuum assistant, the best stacking sequence was $[W/M/W/M]_S$ combination. As similar with mode I test results, the vacuum assistance method still has a positive influence in mode II fracture toughness.

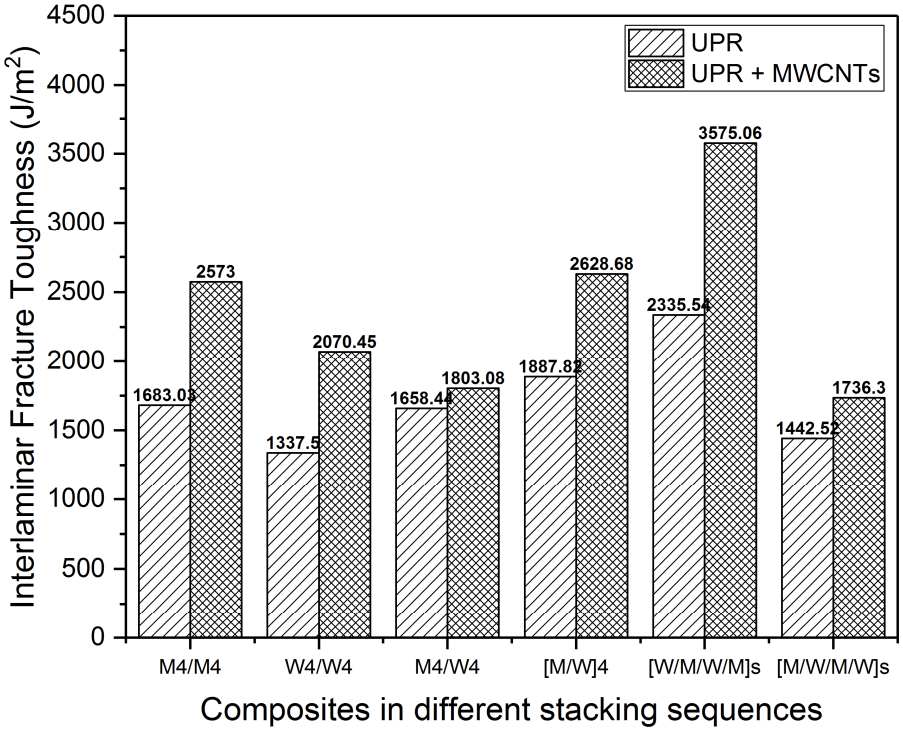

(b) MWCNTs effect on mode II fracture toughness

Figure 3-13(b) presents the different trend comparing with mode I test results, but the MWCNTs kept the strong effect on mode II fracture toughness. The combination of

$[W/M/W/M]_S$ possessed the highest value (3575.06 J/m^2). $[M/W/M/W]_S$ shows the lowest fracture toughness value in all stacking sequences (1736.30 J/m^2). Despite this, the MWCNTs still shows a strong influence on all the specimens. Each of the samples has achieved significantly higher fracture toughness value. The $[M_4/W_4]$ increased 8.72% that is the lowest, $[M_4/M_4]$, $[W_4/W_4]$ and $[M/W]_4$ increased 52.88%, 54.8%, 39.24% separately in mode II fracture toughness. Others' fracture toughness values as follows: $[M/W]_4$ (2628.68 J/m^2), $[M_4/M_4]$ (2573.0 J/m^2), $[W_4/W_4]$ (2070.45 J/m^2), $[M_4/W_4]$ (1803.08 J/m^2).

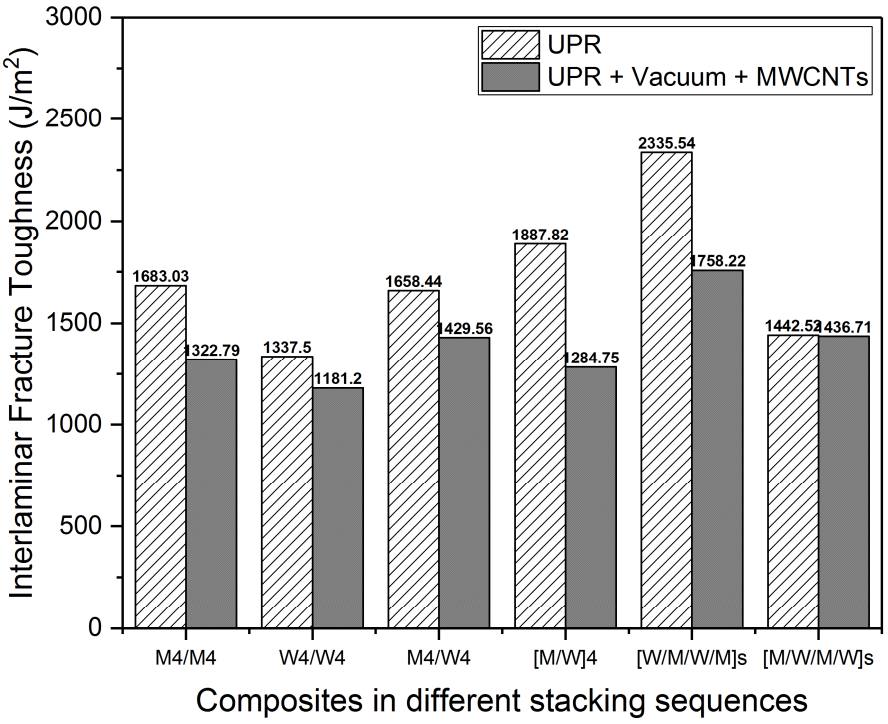

(c) Vacuum & MWCNTs effect on mode II fracture toughness

Figure 3-13: Mode II fracture toughness of composites

The order of fracture toughness for the vacuum & MWCNTs effect is as follows: $[W/M/W/M]_S$ (1758.22 J/m^2), $[M/W/M/W]_S$ (1436.71 J/m^2), $[M_4/W_4]$ (1429.56 J/m^2), $[M_4/M_4]$ (1322.79 J/m^2), $[M/W]_4$ (1284.75 J/m^2) and $[W_4/W_4]$ (1181.20 J/m^2). It could be clearly observed that the fracture toughness for each of stacking sequence decreased from Figure 3-13(c). The reason for this was the increasing flexural modulus of composites. Table

3-1 showed the flexural modulus for each specimen. Under the vacuum assistant and MWCNTs effect, all the stacking sequence samples obtained higher flexural modulus, which means current specimens had a lower ability of deformable resistance during the material elastic limitation. However, the crack propagation was not considered in mode II fracture test. Thus, the samples were only broken locally after test (Figure 3-14).

Table 3-1: Flexural modulus of composites (GPa)

	UPR	UPR + Vacuum	UPR+MWCNTs	UPR + Vacuum + MWCNTs
M_4/M_4	8.73	9.14	7.74	13.03
W_4/W_4	18.97	18.13	16.87	19.90
M_4/W_4	11.68	12.02	11.79	14.48
$【M/W】_4$	12.56	11.61	9.82	15.65
$【W/M/W/M】_S$	16.09	14.02	12.40	17.48
$【M/W/M/W】_S$	16.25	11.28	10.54	17.81

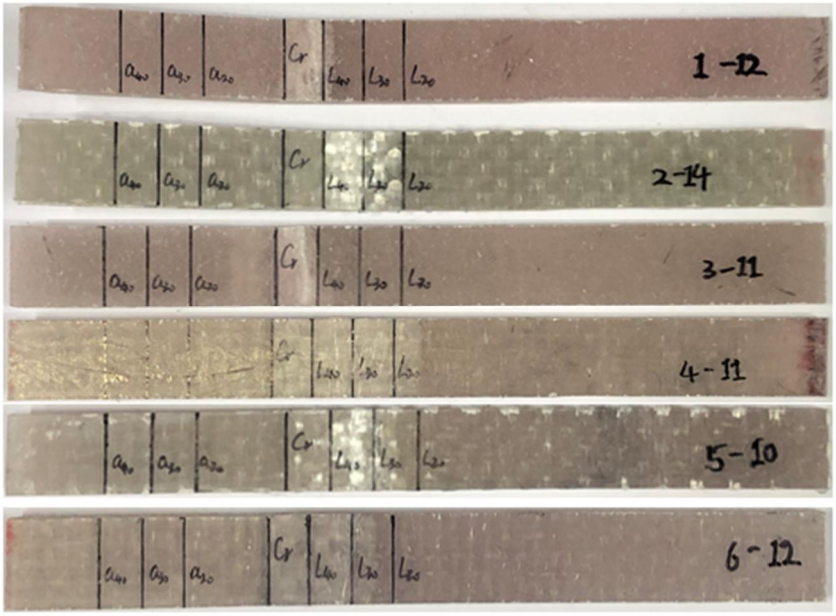

Figure 3-14: The samples after mode II test

For the only chopped strand mat and only woven glass fiber samples, the results were similar with mode I results that woven still presents smaller value comparing with chopped strand mat, which means woven had smaller in-plane shear resistance ability in the center

layer. $[W/M/W/M]_S$ had the highest mode II fracture toughness value during all the composites structure, it showed the toughest materials, and $[W_4/W_4]$ center layer combination had smallest in-plane shear resistance ability among others. In comparison with mode I interlaminar fracture toughness, all of the stacking sequences could relatively undergo higher mode II fracture loading except under vacuum & MWCNTs fabrication condition.

3.4.3 Mode I & mode II relations

Table 3-2: Fracture toughness ratio of mode II/mode I

G_{IIC}/G_{IC}		UPR	UPR + Vacuum	UPR + MWCNTs	UPR+ Vacuum + MWCNTs
1	M_4/M_4	2.93	2.58	3.65	1.53
2	W_4/W_4	2.43	2.56	2.51	1.43
3	M_4/W_4	2.53	2.09	2.08	1.74
4	$[M/W]_4$	3.01	3.48	3.41	1.79
5	$[W/M/W/M]_S$	3.31	3.19	4.52	2.01
6	$[M/W/M/W]_S$	2.56	2.66	2.55	2.12

From Table 3-2, we could find the ratio of G_{IIC}/G_{IC} is larger than 1, which means that each of these stacking sequences could yield higher toughness than mode I fracture toughness. If the G_{IIC}/G_{IC} ratio of some stacking sequences is larger, it means this kind of structure could withstand bigger shear stress. So for some specific parts were broken under lager shear stress, it should be chosen that the stacking sequence has a larger G_{IIC}/G_{IC} ratio.

From these four fabrication conditions, we want to find which one is the best fabrication condition. All of them used UPR as the matrix, so the only UPR fabrication condition group will be used as a standard group to compare with others. So in Figure 3-15, the x-axis is the G_{IIC}/G_{IC} ratio of only UPR fabrication condition, the Y-axis is other fabrication conditions' G_{IIC}/G_{IC} ratio. By using the linear regression equation, we could obtain the slope of the vacuum assisted, MWCNTs and vacuum & MWCNTs combined fabrication conditions.

The slope value showed the effect of each fabrication condition so it could be used as an

indicator to check which fabrication condition has a strong influence compared with the standard group (only UPR fabrication condition). It will illustrate the effect of most structures under the fabrication condition, but it could not represent all of them. If the slope is larger than 1, it means that this kind of condition could significantly enhance the matrix and strongly impacted the fracture toughness, and this fabrication condition will be superior to use during fabrication. If the slope is larger than 0 but smaller than 1, it means that even the fabrication condition still has a positive effect to get a higher fracture toughness, it will not increase too much. The slope could only indicate the effect of fabrication conditions during fracture tests, however, it couldn't represent all the mechanical properties for these fabrication conditions.

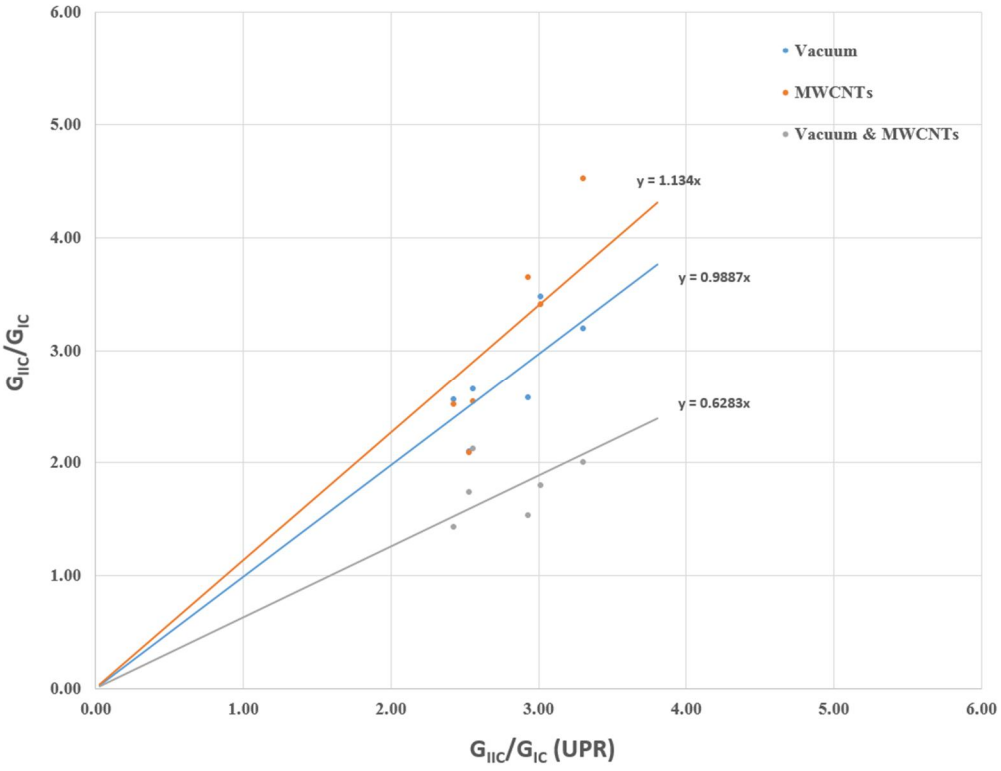

Figure 3-15: G_{IIC}/G_{IC} ratio of other fabrication conditions compared with only UPR fabrication condition

From Figure 3-15, we can see that only the MWCNTs fabrication condition group has the slope larger than 1, which means the MWCNTs could significantly increase the fracture

toughness to a higher value for most structures compared with only UPR fabrication condition, and it was also shown in the above figures about the fracture toughness. The other two groups have the slope smaller than 1 which means even these two fabrication conditions had a positive effect on fracture toughness, it will not increase too much for most structures.

3.5 Conclusions

In this chapter, the mode I and mode II fracture behavior of various glass fibers reinforced UPR composites were investigated in different fabrication conditions. For the UPR only and the vacuum assistant fabrication condition, $[W/M/W/M]_S$ had the best performance in both mode I and mode II fracture test. $[M_4/W_4]$ was the suitable sequence in MWCNTs mixing into UPR fabrication condition. For the combined fabrication condition (vacuum & MWCNTs), the stacking sequence $[W/M/W/M]_S$ was the best choice among all cases. Considering the performance and fracture toughness value, $[W/M/W/M]_S$ with the MWCNTs fabrication condition is recommended for all the cases and conditions. In consequence, the mode I and mode II interlaminar fracture toughness value of MWCNTs fabrication group was found that adding MWCNTs in the composite matrix was an effective method. The vacuum assistant was also an economic method to improve composite fracture toughness. In all the cases of stacking sequences, mode II fracture toughness is higher than mode I values.

CHAPTER 4:

Conclusions and future work

4.1 Conclusions

In this thesis, the mechanical properties and mode I, mode II fracture behavior of various glass fibers reinforced UPR composites were investigated in different fabrication conditions. For the experimental fabrication conditions, applying vacuum had a positive influence on the density, thickness, mass and tensile properties of composites. MWCNTs also possessed a good effect on the tensile properties of composite structure.

The stacking sequence strongly impacted the mechanical properties of fiber-reinforced composites. The $[W_4/W_4]$ combination under vacuum & MWCNTs fabrication condition had a higher density, smaller thickness and light weight, and $[W/M/W/M]_S$ with the MWCNTs fabrication condition had a higher fracture toughness during all the cases, also $[W/M/W/M]_S$ showed a very close to the mechanical properties of $[W_4/W_4]$. As for industry applications, applying vacuum is a simple and effective method to get lighter and higher mechanical properties composites products. In some parts that aim to withstand high strength, adding MWCNTs is a good way to achieve goals.

4.2 Future works

Currently, the $[W/M/W/M]_S$ combination was the best choice of the laminated composite based on several factors (density, thickness, mass, tensile properties and mode I, mode II fracture toughness). All of results in this thesis are experiment results, the basic parameters such as Young's modulus and Poisson's ratio were obtained which could be helpful for the future simulation work. The mixed mode behavior will be used to study previous conclusion and the interlayer reactions and failure criterion of composite laminates also should be considered during the finite element analysis, either. By fully considering the experiment results and finite element analysis results, laminated composites could be reliable of the future industrial application.

REFERENCE

[1] Fazeli, Mahyar, Jennifer Paola Florez, and Renata Antoun Simão. "Improvement in adhesion of cellulose fibers to the thermoplastic starch matrix by plasma treatment modification." *Composites Part B: Engineering* 163 (2019): 207-216.

[2] Elhajjar, Rani, Valeria La Saponara, and Anastasia Muliana, eds. *Smart Composites: Mechanics and Design*. CRC Press, 2013.

[3] Johnson, Todd. "History of Composites: The Evolution of Lightweight Composite Materials." *About Money, [Online]. Available: http://composite. about. com/ od/ about composite splastics/ a/ HistoryofComposites. htm.* [Accessed 18 Oct 2014] (2017).

[4] Jang, Bor Z. "Advanced polymer composites: principles and applications." *ASM International, Materials Park, OH 44073-0002, USA, 1994*. 305 (1994).

[5] Álvarez, Vera, et al. "The influence of matrix chemical structure on the mode I and II interlaminar fracture toughness of glass-fiber/epoxy composites." *Polymer composites* 24.1 (2003): 140-148.

[6] Modrea, Arina, Florin Teodorescu, and Dorin Rosu. "Tensile Tests on Four Layers CSM600 Glass Fibers-reinforced Polylite 440-M888 Polyester Resin." *Procedia Technology* 19 (2015): 284-290.

[7] Jones, Robert M. *Mechanics of composite materials*. CRC press, 2014.

[8] Ashby, Michael F., and D. Cebon. "Materials selection in mechanical design." *Le Journal de Physique IV* 3.C7 (1993): C7-1.

[9] Kelly, Anthony, and Carl H. Zweben. *Comprehensive composite materials*. Elsevier, 2000.

[10] Iijima, Sumio. "Helical microtubules of graphitic carbon." *Nature* 354.6348 (1991): 56.

[11] Chand, S. "Review carbon fibers for composites." *Journal of materials science* 35.6 (2000): 1303-1313.

[12] Huang, Xiaosong. "Fabrication and properties of carbon fibers." *Materials* 2.4 (2009): 2369-2403.

[13] Beg, M. D. H., et al. "Improvement of interaction between pre-dispersed multi-walled carbon nanotubes and unsaturated polyester resin." *Journal of Nanoparticle Research* 17.1 (2015): 53.

[14] Shokrieh, Mahmoud M., Ali Saeedi, and Majid Chitsazzadeh. "Mechanical properties of multi-walled carbon nanotube/polyester nanocomposites." *Journal of Nanostructure in Chemistry* 3.1 (2013): 20.

[15] Guo, Peng, et al. "Fabrication and mechanical properties of well-dispersed multiwalled carbon nanotubes/epoxy composites." *Composites science and Technology* 67.15-16 (2007): 3331-3337.

[16] Montazeri, Arash, et al. "Mechanical properties of multi-walled carbon nanotube/epoxy composites." *Materials & Design* 31.9 (2010): 4202-4208.

[17] Hoang, Van-Tho, Jin Young Kim, and Young Jin Yum. "Tensile Properties of Multi-walled Carbon Nanotubes/Unsaturated Polyester Resin Mixing by Stir Method." *Proceedings of KSME Conference* (2016): 2416-2418.

[18] Tian Gou, and Yum, Young-Jin. "The effect of stacking sequence and vacuum on mode I fracture toughness of glass fiber reinforced unsaturated polyester resin composites," *Proceedings of KSME Conference* (2019).

[19] Seong, Dong Gi, et al. "Influence of fiber length and its distribution in three phase poly (propylene) composites." *Composites Part B: Engineering* 168 (2019): 218-225.

[20] Hoang, Van-Tho, and Yum, Young-Jin, "Optimization of the fabrication conditions and effects of multi-walled carbon nanotubes on the tensile properties of various glass fibers/unsaturated polyester resin composites," *e-Polymers*, 18.5(2018): 441-451.

[21] Hennigan, Daniel John, and Kevin Daniel Beavers. "Effect of fabrication processes on mechanical properties of glass fiber reinforced polymer composites for 49 meter (160 foot) recreational yachts." *International Journal of naval architecture and ocean engineering* 2.1 (2010): 45-56.

[22] Caprino, G., J. C. Halpin, and L. Nicolais. " Fracture toughness of graphite/epoxy laminates." *Composites* 11.2 (1980): 105-107.

[23] Harris, B., S. E. Dorey, and R. G. Cooke. "Strength and toughness of fibre composites." *Composites science and technology* 31.2 (1988): 121-141.

[24] Chai, H. "The characterization of mode I delamination failure in non-woven, multidirectional laminates." *Composites* 15.4 (1984): 277-290.

[25] Madhukar, Madhu S., and Lawrence T. Drzal. "Fiber-matrix adhesion and its effect on composite mechanical properties: IV. Mode I and mode II fracture toughness of graphite/epoxy composites." *Journal of Composite Materials* 26.7 (1992): 936-968.

[26] CHARENTENAY, DE. "Delamination of glass fiber reinforced polyester, an acoustic emission study." *Mechanical behaviour of materials* (1980): 241-251.

[27] Bascom, W. D., et al. "The interlaminar fracture of organic-matrix, woven reinforcement composites." *Composites* 11.1 (1980): 9-18.

[28] CHARENTENAY, DE. "Fracture mechanics of Mode I delamination in composite materials." *Advances in composite materials* (1980): 186-197.

[29] Seyhan, A. Tugrul, Metin Tanoglu, and Karl Schulte. "Mode I and mode II fracture toughness of E-glass non-crimp fabric/carbon nanotube (CNT) modified polymer based composites." *Engineering Fracture Mechanics* 75.18 (2008): 5151-5162.

[30] Rikards, R., et al. "Mode I, mode II, and mixed-mode I/II interlaminar fracture toughness of GFRP influenced by fiber surface treatment." *Mechanics of composite materials* 32.5 (1996): 439-462.

[31] Yum, Young-Jin, and Hee You. "Pure mode I, II and mixed mode interlaminar fracture of graphite/epoxy composite materials." *Journal of reinforced plastics and composites* 20.9 (2001): 794-808.

[32] Zou, Peng, et al. "Mode I delamination mechanism analysis on CFRP interference-fit during the installation process." *Materials & Design* 116 (2017): 268-277.

[33] Fernandes, R. L, M. F. S. F. De Moura, and R. D. F. Moreira. "Effect of moisture on pure mode I and II fracture behaviour of composite bonded joints." *International Journal of Adhesion and Adhesives* 68 (2016): 30-38.

[34] Rao, D. Srikanth, P. Ravinder Reddy, and Sriram Venkatesh. "Determination of mode-I fracture toughness of epoxy-glass fibre composite laminate." *Procedia engineering* 173 (2017): 1678-1683.

[35] Holdsworth, A. W., S. Morris, and M. J. Owen. "The fracture toughness of a glass chopped-strand-mat/polyester-resin laminate." *Journal of Physics D: Applied Physics* 7.15 (1974): 2036.

[36] Navarro, Pablo, et al. "Effects of the Stacking Sequence, Material Nature and Addition of an Adhesive Film on the Delamination Resistance of Woven Composite Laminates in Mode I and II." *Advanced Composites Letters* 24.1 (2015).

[37] Fuoss, Edgar, Paul V. Straznicky, and Cheung Poon. "Effects of stacking sequence on the impact resistance in composite laminates. Part 2: prediction method." *Composite Structures*41.2 (1998): 177-186.

[38] Park, J. H., et al. "Stacking sequence design of composite laminates for maximum strength using genetic algorithms." *Composite Structures* 52.2 (2001): 217-231.

[39] Davidson, B. D., R. Krüger, and M. König. "Effect of stacking sequence on energy release rate distributions in multidirectional DCB and ENF specimens." *Engineering Fracture Mechanics* 55.4 (1996): 557-569.

[40] ASTM D5528-13. Standard test method for mode I interlaminar fracture toughness of unidirectional fiber-reinforced matrix composites. *ASTM International, West Conshohocken, PA*; 2013.

[41] ASTM D7905-14. Standard test method for determination of the mode II interlaminar fracture toughness of unidirectional fiber-reinforced polymer matrix composites. Space simulation; aerospace and aircraft; composite materials. *ASTM International, West Conshohocken*, PA; 2015.

[42] Ding W. Delamination analysis of composite laminates. University of Toronto; 2000.

[43] Bao-Zong Huang, Li-Jun Zhao, 2012, “Bridging and toughening of short fibers in SMC and parametric optimum.” *Composites: Part B*, Vol. 43, pp. 3146~3152.

[44] L.P. Canal, G. Pappas, J. Botsis, 2016, “Large scale fiber bridging in mode I interlaminar fracture. An embedded cell approach.” *Composites Science and Technology*, Vol. 126, pp. 52~59.